UNIVERSITY OF CALIFORNIA
RIVERSIDE

Addressing Key Unanswered Questions Regarding the Mechanism of Ethylene Hydrogenation on Pt Single Crystals

A Dissertation submitted in partial satisfaction
of the requirements for the degree of

Doctor of Philosophy

in

Chemistry

by

Juan Pablo Simonovis

December 2015

Dissertation Comittee:
Dr. Francisco Zaera, Chairperson
Dr. Leonard Mueller
Dr. Jingsong Zhang

The Dissertation of Juan Pablo Simonovis is approved:

_____

_____

_____
Committee Chairperson

University of California, Riverside

ACKNOWLEDGEMENTS

I would like to thank Dr. Francisco Zaera for giving me the unique opportunity to join his group and work with the advanced systems in his laboratory. I am grateful for his valuable advice, his professionalism and his unique take in science, asking the fundamental questions in chemistry that are commonly overlooked in this time and age due to their lack of short term application but that are nonetheless invaluable to expand the understanding of everyday chemical systems.

As always, words are not enough to express my thanks for the unconditional support provided by my parents despite the distance: My mother always the perfect example of patience and wisdom. She is the constant reminder that a kind heart and open mind are crucial in the upbringing of an individual. My father, the constant example of persistence and hard work. I also need to mention my surrogate father, Homero Navas for teaching me that humor and fun are just as important in any life endeavor as hard work.

To my siblings, Leonora and Alejandro and their corresponding families for their care, attention and support.

To Dr. Carmelo Bolivar for guiding me in becoming an independent scientist and teaching me that you always have to be as big as the challenge.

I am grateful to Stanley Sheldon for his invaluable advice and assistance during the design and construction of the circulation loop which was crucial to this work. I am also thankful to my lab mates in the Zaera Group for their constant support and guidance. A special thanks to Dr. Ilkeun Lee for solving what at the moment seemed unsolvable.

A special thanks to the Aikido Family at UCR for providing unique experiences outside of school and allowing me to expand my knowledge and skills in a life path that I started almost 18 years ago.

I would like to thank the staff at the chemistry department: Prisciliano Saavedra, Tina Enriquez, Christina Youhas, Barbara Outzen and Jaime Matute and the staff at the physics machine shop for always solving issues in a timely manner.

Finally, I would like to thank Touba for her irreplaceable companionship.

Part of the results from the fourth chapter of this thesis were published in *ACS Catalysis* (DOI 10.1021/cs300411p), while part of the results of chapter six were reported in the *Journal of Physical Chemistry Letters* (DOI: 10.1021/jz500954g).

ABSTRACT OF THE DISSERTATION

Addressing Key Unanswered Questions Regarding the Mechanism of Ethylene Hydrogenation on Pt Single Crystals

by

Juan Pablo Simonovis

Doctor of Philosophy, Graduate Program in Chemistry
University of California, Riverside, December 2015
Dr. Francisco Zaera, Chairperson

Since its first proposal by Horiuti and Polanyi, the mechanism of the catalytic hydrogenation of ethylene over Pt has been the subject of much debate, and there are some pending questions still regarding the transformations that take place on the surface of the working catalysts. Model studies on ideal transition metal surfaces under ultra-high vacuum (UHV) conditions have allotted very useful information regarding the possible pathways for this reaction. However, past findings from studies with model systems do not always correlate with results obtained under more realistic catalytic conditions.

This work has focused on implementing a recently developed operando setup installed in a UHV chamber to probe some pending questions regarding the mechanism of ethylene hydrogenation, mainly: the role of carbonaceous deposits on the surface, the dissociative adsorption of hydrogen as the rate limiting-step of the reaction, and what is

known as the “pressure gap”. Our results show that the alkylidynes formed during reaction due to the decomposition of the olefin in the gas phase can readily be displaced and hydrogenated at a rate much slower than that of the gas phase olefin, corroborating previous findings. Furthermore, while probing the pressure gap it was found that at low enough ethylene pressures the hydrogenation reaction occurs over a seemingly clean surface with high reaction probabilities.

Additional surprising results were obtained by following the evolution of H-D scrambling during the catalytic hydrogenation of ethylene: The production of HD shows a sharp non-linear transition in its kinetics when the pressure of the olefin in the gas phase is below 1 Torr. This switch in kinetics suggests that during the first stages of the reaction the dissociative adsorption of hydrogen on the metal surface is the rate-limiting step. However, after the transition this is no longer the case. This discovery represents compelling evidence of the existence of two well-defined kinetic regimes during the hydrogenation of ethylene over Pt (111) single crystals.

TABLE OF CONTENTS

LIST OF FIGURES

CHAPTER 1: INTRODUCTION.

The catalytic hydrogenation of ethylene over transition metals has been one of the most widely studied systems since its discovery by Sabatier and Sanderens in 1897 [1]. It requires mild reaction conditions (atmospheric pressures, ~ 200 C), and the molecules involved in the process are simple and have been characterized in detail. For these reasons, it has been considered a suitable reaction for experimental and theoretical modeling.

Despite extensive studies in the past century, the mechanism that describes this reaction has not been fully elucidated and is still the subject of much debate. Like in any hydrogenation process, the kinetics involved suffer from a series of limitations, mainly determining the variety of possible adsorbed forms of the hydrocarbon and the sensitivity to small changes in temperature and pressure conditions [2]. The first researchers that confected a mechanism based on experimental findings were Horiuti and Polanyi [3] in 1934. The basic features of the reaction pathway shown in Figure 1.1, include the dissociative adsorption of hydrogen on the surface of the catalyst, the chemisorption of ethylene as a di-σ bonded species, and the step by step addition of adsorbed hydrogen to the di-σ ethylene going through an ethyl intermediate to give the final product, ethane. This mechanism was strongly challenged [4], since there were different views on how the species involved interacted with each other, and the time-dependent decrease of reaction rates suggested that the reaction did not occur over a clean surface. It was believed that the decomposition of olefins led to the deposition of strongly bonded carbonaceous

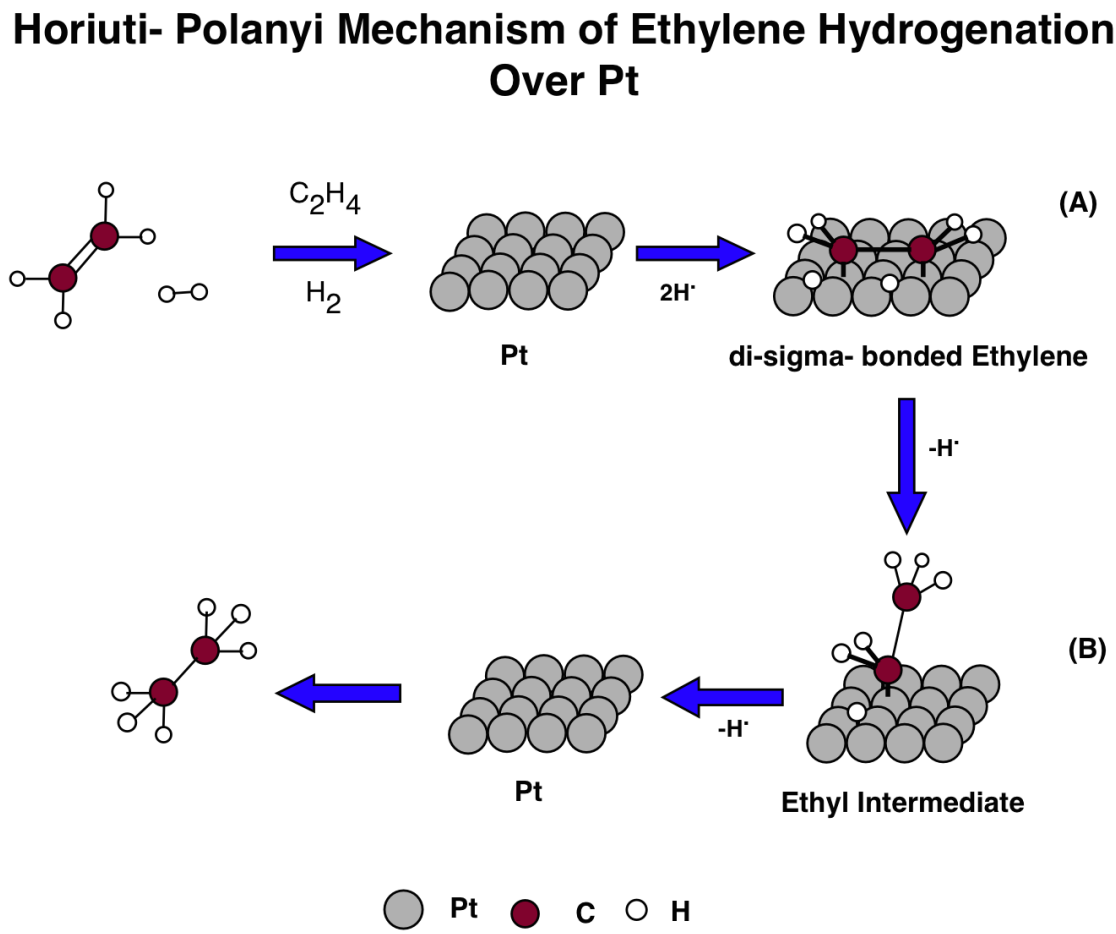

Figure 1.1. Basic features of the Horiuti-Polanyi mechanism for ethylene hydrogenation: (A) Formation of the di-σ bonded ethylene and dissociative adsorption of hydrogen. (B) Formation of ethyl intermediate.

species on the surface [4]. Research done on this system was based either on metallic foils or supported transition metal catalysts (Ni, Pd, Pt, Re, Rh) [5] under conditions that were very similar to the ones used in industrial processes. This approach, although needed, is very complex from the kinetics point of view and enhances the difficulty of identifying microscopic reaction steps.

The complexity of catalytic studies carried under realistic conditions has been somewhat circumvented by the use of ultra high vacuum (UHV) systems that allow the use of single crystalline surfaces under a very controlled environment which guarantees the absence of contaminants [6]. However, as was recognized early on, there is no direct correlation between the chemistry identified by vacuum surface-sensitive techniques and the reactions that take place under atmospheric or high pressures. This issue is referred to as the *pressure gap* [5]. Regardless of this limitation, research carried out under UHV [6] conditions has added to the understanding of the interaction between molecules and surfaces, their adsorption properties, and dynamics. In terms of chemical kinetics, it has helped elucidate some elementary steps in catalytic reactions, affording a better understanding of their mechanism.

Ultra high vacuum studies of the catalytic hydrogenation of C_2H_4 over single crystals have employed, among other surface-sensitive techniques, infrared spectroscopy (IR) [7], high-resolution electron energy loss spectroscopy (HREELS) [8], and sum frequency generation (SFG) [9] to identify the surface intermediates involved in the hydrogenation process. These studies show that three stable surface species are found during the reaction: π-bonded C_2H_4, di-σ bonded ethylene, and ethylidyne (C_2H_3). The π-

bonded species is stable at temperatures below 52 K [10]. It interacts with the metal surface through the π electron cloud with very little structure change. Above 52 K one of the C-C bonds breaks, generating two σ bonds with the metal surface, resulting in a di-σ bonded ethylene species that is face-centered cubic (fcc) in a three fold hollow site with the C-C bond tilted up slightly with respect to the surface plane [11]. At 240 K this specie decomposes, loosing one hydrogen atom and transferring another to the adjacent carbon forming C_2H_3. Ethylidyne is bonded to three Pt atoms from the surface and resides in a fcc three-fold hollow site. At 300 K this hydrocarbon moiety is very stable and shows great mobility, thanks to which the hydrogenation of ethylidyne is several orders of magnitude slower than the hydrogenation of gas phase ethylene [12] -excluding it as a reaction intermediate. This lack of reactivity explains why at 300 K and under UHV conditions -where a limited amount of hydrogen is available on the surface- the catalytic hydrogenation of C_2H_4 is not sustained [13].

Some UHV systems have been fitted with small reactors [14, 15, 16] inside the vacuum environment for the isolation of the metal sample so it can be exposed to high-pressure gas mixtures (~700 Torr) without loosing vacuum conditions. Coupling the reactor with analytical techniques such as gas chromatography (GC) or mass spectrometry (MS), it is possible to follow the kinetics of the hydrogenation reaction and, depending on the setup, vibrational spectroscopies and others [17], can also be used to monitor *in situ* the species that are generated on the surface during the process [9, 15]. Results obtained with these types of instruments have shown that the rate C_2H_4 hydrogenation is, within the accuracy of those experiments, insensitive [18] to the

structure of the metal surface. For instance, studies carried out over Pt (111) and Pt (100) showed that, for a mixture of 32 Torr of C_2H_4 and 100 Torr of H_2, the turnover frequencies for the reaction are 11 and 12 C_2H_6 molecules Pt site^{-1}s^{-1}, respectively [19]. It was also proven that under these reaction conditions, ethylene readily dehydrogenates on the clean metal surface to form adsorbed ethylidyne (Figure 1.2) instead of hydrogenating to ethane. This strongly bonded species is present during and after reaction [15]. Both IR and SFG *in situ* studies [9] carried out at high pressures also confirmed the presence of the π-bonded C_2H_4 and di-σ bonded ethylene as surface species involved in the catalytic hydrogenation of ethylene. These and other observations have provided insight into the catalytic hydrogenation of ethylene; however, they are still far from providing a complete and concise mechanism.

As stated previously, modern surface science has provided more detail in regards to the mechanism of ethylene hydrogenation. Nonetheless, it has also uncovered the complexity of the reaction, raising more questions that need to be answered, among which are: the role of the carbonaceous deposits, the adsorption of hydrogen as the rate-limiting step and the pressure gap. These three main topics will be addressed in this thesis.

1.1. The role of the carbonaceous deposits.

It is still not clear what role the carbonaceous deposits play in the hydrogenation process. It has been suggested that these species might store hydrogen, releasing it during reaction either through direct exchange or by transferring hydrogen atoms from the metal surface to a second layer of physisorbed ethylene [5]. *In situ* studies have shown that the

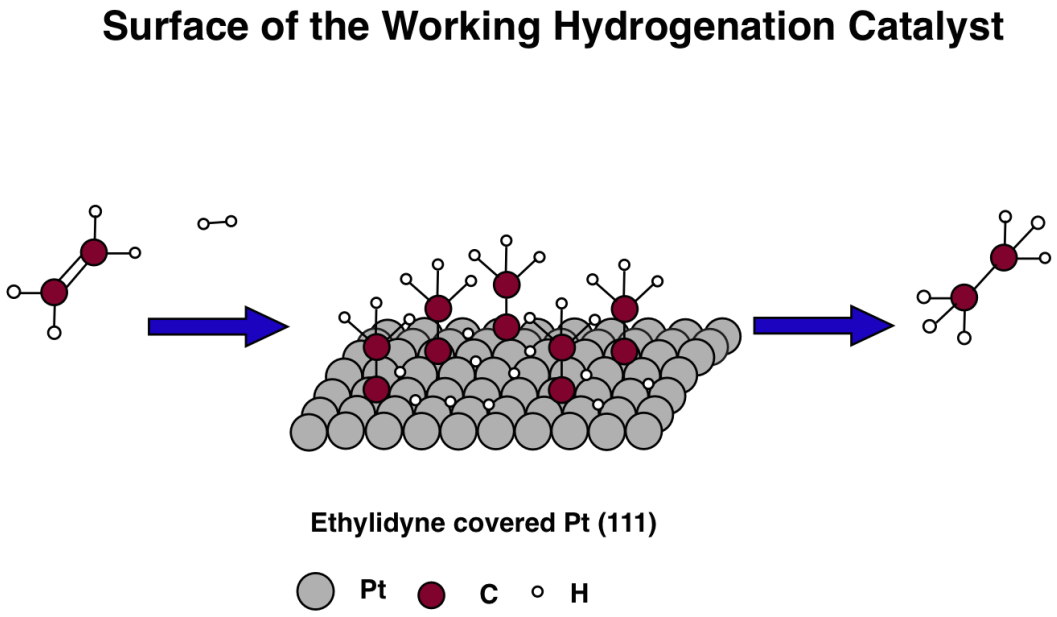

Figure 1.2. Representation of the surface of the working hydrogenation catalyst. During the catalytic conversion of ethylene to ethane the surface is covered with strongly bonded hydrocarbon deposits, namely ethylidyne.

rate of H-D exchange of ethylidyne layers during the catalytic hydrogenation is approximately 1 x 10^{-5} MLs^{-1}, too slow to facilitate ethylene hydrogenation. Shuttling hydrogen from the metal surface to the physisorbed ethylene layer might be possible through an alkylidene intermediate. This moiety has been isolated and identified in vacuum [20, 21] and detected during the conversion of ethylene to ethylidyne [22, 23]. At high hydrogen pressures the steady-state surface coverage of this hydrogen shuttling intermediate is expected to be low, and the vibrational features that identify it are predicted to be weak, so there is currently no evidence to prove that the carbonaceous layer present on the surface during the catalytic hydrogenation has the ability to transfer hydrogen to a second layer of adsorbed ethylene.

It has also been suggested that the alkylidyne moieties present on the surface during the catalytic hydrogenation of ethylene also condition the reactivity of the bare metal, promoting weak olefin adsorption and hydrogenation. Previous studies have shown that under high-pressure conditions, the surface is almost completely saturated with these hydrocarbon deposits, blocking almost every available platinum site and possibly favoring π-bonded ethylene, which is considered to be the most likely intermediate for the reaction [24]. But at the same time it might hinder the formation of ethyl intermediates and adsorbed hydrogen. It is speculated that an equilibrium between ethylidyne and a proposed ethylidene intermediate might be responsible for the surface mobility of ethylidyne, which might, in turn, open the surface sites needed for catalysis. Nevertheless, no proof has been found to substantiate this claim.

1.2. Hydrogen adsorption as the rate-limiting step.

Another question that has gone unresolved -and that is directly related to the presence of the carbonaceous deposits- is that of the hydrogen intake by the olefin during the catalytic hydrogenation of ethylene. It is well accepted [5] that olefin hydrogenation requires both reactants to be adsorbed on the surface- following a Langmuir-Hinshelwood mechanism- and that the reactive species is atomic, not molecular, hydrogen. Conversely, the strongly bonded hydrocarbon deposits that form readily during the catalytic reaction, block the bare metal sites needed for olefin conversion. This might explain why the catalytic hydrogenation is not sustained under UHV conditions. However, in experiments at atmospheric pressures, where there is a constant supply of hydrogen, a steady-state coverage of bare metal sites is found to be responsible for hydrogen and olefin adsorption [5]. It is worth mentioning that olefin hydrogenation catalysis displays first order dependence on hydrogen pressure [25, 26], which suggests that the dissociative adsorption of hydrogen may be the rate-limiting step. Given that a layer of hydrocarbons covers the surface of the working catalysts, the concentration of surface hydrogen is expected to be low and its mobility partially blocked. This has been shown by isotope labeling experiments carried out under vacuum that showed limited deuterium incorporation [23, 27]. Presently, despite these findings, the kinetics of hydrogen uptake during the catalytic hydrogenation of olefins is not well understood.

1.3. The pressure gap.

As mentioned before, surface-science studies showed that there are fundamental differences between experiments carried out over ideal surfaces under UHV conditions,

and those carried out over supported catalysts. Two main pressure regimes have been identified [5]:

- Pressures bellow 1 x 10^{-6} Torr: Hydrogenation can occur over transition metal surfaces that have been pre-covered with hydrogen but catalysis is not sustained.
- Pressures above 1 Torr (atmospheric pressures): catalysis is sustained in a steady state fashion, over a surface that is heavily covered with hydrocarbon deposits.

The kinetic evidence obtained seems to suggest that the mechanisms or the rate-limiting step that occur in each pressure regime are different, since the hydrogenation of ethylene is first order in both hydrogen and the olefin under UHV conditions [28], and first order in hydrogen but close to zero order in the olefin at atmospheric pressures [14]. This implies that a shift in mechanism may need to happen in the intermediate pressure range between 1x 10^{-6} Torr and 1 Torr.

The turnover frequencies (TOF) for ethylene hydrogenation tend to be high even at room temperature, as stated previously. However they still represent reaction probabilities in the range between 1x 10^{-6} and 1x 10^{-5}. These reaction probabilities increase with decreasing olefin pressures since the hydrogenation rate is zero order on the olefin under high-pressure conditions. Near unity probabilities are found at pressures around 1x 10^{-6} to 1x 10^{-4} Torr [29]. This trend predicts that at olefin pressures like the ones used in UHV studies, the probability would be greater than one: not only does that lack any physical meaning, but results show that almost no catalytic reactivity is detected

under those conditions. The lack of kinetic information available regarding the intermediate pressure regime needs to be addressed in order to obtain a complete understanding of the reaction mechanism for the catalytic hydrogenation of ethylene and olefins in general.

To explore these issues, my study relied on the use of a recently developed operando setup. Its main feature was a well-stirred batch reactor located inside an ultra-high vacuum chamber that allowed performing catalytic hydrogenation of ethylene at atmospheric or near atmospheric pressures without jeopardizing the vacuum environment. This arrangement enabled the mass spectrometric analysis of evolved gas phase species, and the spectroscopic inspection of surface moieties during the catalytic reaction.

This thesis is comprised of 7 chapters, starting with an overview of previous findings that support my research (Chapter 1). Chapter 2 offers a discussion of the experimental approach, instrumentation, and surface-sensitive techniques used in this work. Chapter 3 describes the generic hydrogenation experiment. Chapter 4 addresses the chemistry involved in the catalytic hydrogenation of ethylene over a Pt (111) surface covered with strongly bonded hydrocarbon deposits. Chapter 5 studies the dissociative adsorption of hydrogen as the rate-limiting step of the hydrogenation reaction of ethylene over Pt. The findings of this chapter offer an undocumented behavior of the H-D exchange reaction during the hydrogenation of ethylene and represent the most compelling discovery of my work. Chapter 6 attempts to deal with the pressure gap explained earlier by performing catalytic reactions with super diluted gas mixtures where

the olefin pressures are in the mTorr range. The documentation of this research is brought to a close with some general conclusions and suggestions for future work (Chapter 7).

1.4. References.

[1] P. Sabatier and J.-B. Senderens, *C. R. Hebd. Seances Acad.Sci.*, **1897**, 1358.

[2] Cerveny, L, *Studies in Surface Science and Catalysis 27: Catalytic Hydrogenation, Elsevier,* **1986.**

[3] M. Polanyi and J. Horiuti, *Trans. Faraday Soc.*, **1934**, 30, 1164.

[4] Jenkins, G. I.; Rideal, E., *J. Chem. Soc.* **1955**, 2490-2496.

[5] Zaera F., *Phys. Chem. Chem. Phys* **2013**, 15, 11988-12003.

[6] Dwyer, D.J., Hoffman, F.M., American Chemical Society. Division of Collois and Surface Chemistry. American Chemical Society. Meeting, *Surface Science of Catalysis: in situ probes and reaction kinetics*, American Chemical Society, Washington, D.C., **1992**, p. xii, 364 p.

[7] Kubota, J.; Ohtani, T.; Kondo, J.N.; Hirose C.; and Domen, K., *Appl. Surf. Sci.*, **1996**, 122, 548-551.

[8] Skinner, P.; Howard, M.W.; Oxton, I.A.; Kettle, S.F.A.; Powell, D.B.; Shepard N., *J. Chem. Soc., Faraday Trans. II* **1981**, *77*,1203-1215.

[9] Cremer, P. S.; Su, X.; Shen, Y. R.; Somorjai, G. A., *J. Am. Chem. Soc.* **1996**, *118*, 2942-2949.

[10] Cassuto, A.; Kiss, J.; White, J.M., *Surf. Sci.* **1991**, *255*, 511.

[11] Doll, R.; Gerken, C.A.; Van Hove, M.A.; Somorjai, G.A., *Surf. Sci.*, **1997**, *374*, 151-161.

[12] Davis, S. M.; Zaera, F.; Gordon, B.; Somorjai, G. A., *J. Catal.* **1985**, *92*, 240-246.

[13] Salmerón, M. and Somorjai, G.A., *J. Phys. Chem*., **1982**, 86, 341.

[14] Ohtani T.; Kubota, J.; Kondo, J.N.; Hirose, C. and Domen, J., *J. Phys. Chem. B*, **1999**, 103, 4562.

[15] Tillekaratne, A.; Simonovis, J. P.; López Fagúndez, M. F.; Ebrahimi, M.; Zaera, F., *ACS Catal.* **2012**, *2*, 2259-2268.

[16] Zaera, F. and Somorjai, G.A., *J. Am. Chem. Soc*, **1984**, 106, 2288-2293.

[17] Koestner, R. J.; Stohr, J.; Gland, J. L. and Horseley, J. A., *Chem. Phys. Lett.* 105, **1984**, 332

[18] Schlatter, J. C. and Boudart, M., *J. Catal*., **1972**, 24, 482.

[19] Somorjai, G.A. and Li, Y., *Introduction to Surface Chemistry and Catalysis, Second Edition*, Wiley, **2010**, p. 586.

[20] F. Zaera, T. V. W. Janssens and H. Ofner, *Surf. Sci*., **1996**, 368, 371.

[21] T. V. W. Janssens and F. Zaera, *J. Phys. Chem*., **1996**, 100, 14118.

[22] Koel, B.E.; Bent, B.E.; Somorjai, G.A., *Surf. Sci.*, **1984**, *146*, 211.

[23] Janssens, T. V. W.; Stone, D.; Hemminger, J. C.; Zaera, F., *J. Catal.*, **1998**, *177*, 284.

[24] Davis, S.M.; Zaera, F. and Somorjai, G.A., *J. Catal.*, **1982**, 439-459.

[25] Horiuti, J. and Miyahara, K., *Hydrogenation of Ethylene on Metallic Catalysts,* Report NSRDS-NBC No. 13, National Bureau of Standards, Washington, **1968**.

[26] Bond, G. C., *Metal-Catalysed Reactions of Hydrocarbons*, Springer, New York, **2005.**

[27] F. Zaera and D. Chrysostomou, Surf. Sci., **2000**, *457*, 89.

[28] Ofner, H.; Zaera, F., *J. Phys. Chem. B*, **1997**, *101*, 396.

[29] Ebrahimi M.; Simonovis J.P.; Zaera F., *J. Phys. Chem. Lett.* **2014**, 5, 2121-2125.

CHAPTER 2: EXPERIMENTAL.

2.1. Introduction.

In all the chapters of this thesis, experiments were carried out inside an ultra-high vacuum chamber (UHV) equipped with a mass spectrometer (MS) capable of performing Temperature Programed Desorption (TPD) experiments. The system is also aligned with a Reflection-Absorption Infrared Spectroscopy setup that is able to carry out vibrational analysis of the surface species before, during, and after reaction. The UHV chamber is rigged with an internal, well stirred, batch reactor that can be isolated from the vacuum environment to perform experiments at near atmospheric or atmospheric pressures.

2.2. Materials.

A disk-shaped sample of Pt (111), 8 mm in diameter and 2 mm in thickness, was cut and polished by standard crystallographic methods. This disk was mounted on the sample manipulator via spot-welding to a pair of molybdenum wires that are connected to the copper rods from the electrical feedthroughs. This arrangement allowed cooling of the Pt sample to approximately 80 K using a continuous flow of liquid nitrogen, and to be heated resistively to 1100 K. The temperature was measured with a chromel-alumel thermocouple that was spot-welded to the side of the crystal. Prior to each experiment, the sample was routinely cleaned by means of oxidation cycles in $2x10^{-6}$ Torr of oxygen at 700 K and annealing in vacuum to a temperature of 1100 K. The crystal was treated with Ar^{+} sputtering (500 kV, 0.7 mA, 7 min and $3x10^{-6}$ Torr of Ar) only when the

chamber was vented and was opened for repairs. This was done to avoid generating surface defects due to collisions with accelerated Ar^+ ions.

Finally, for all the experiments described in this thesis, the ultrahigh purity oxygen, hydrogen, and argon were supplied by Airgas and used as received. Ethylene, butylene, propylene, and deuterium were supplied by Matheson-Trigas and were employed without any further purification.

2.3. Experimental Apparatus.

All experiments were carried out in a two tier stainless-steel ultra high vacuum [1, 2] chamber (Figure 2.1) that is pumped to a base pressure of 1-2 $x10^{-10}$ Torr by means of a cryo-pump. The main part of this chamber is equipped with a UTI 100C quadrupole mass spectrometer (QMS) retrofitted with a retractable nose cone. The cone ends in a 5 mm in diameter aperture that allows the entry of the molecules present in the gas phase for analysis. This mass spectrometer is interfaced to a personal computer capable of monitoring the time or temperature evolution of up to 15 different masses – simultaneously- in one catalytic experiment. The mass spectrometer signals are reported in arbitrary units, but scales are provided in each figure to allow comparisons.

The second deck of the chamber holds the high-pressure cell (HPC) (Figure 2.2). It can be reached by means of the long travel manipulator and it is used to carry out Reflection Absorption Infrared Spectroscopy (RAIRS) experiments (Figure 2.3). The IR beam of a Bruker Equinox 55 FT-IR spectrometer is polarized and focused through a NaCl window onto the sample at grazing incidence (~85^o). The resulting beam is then

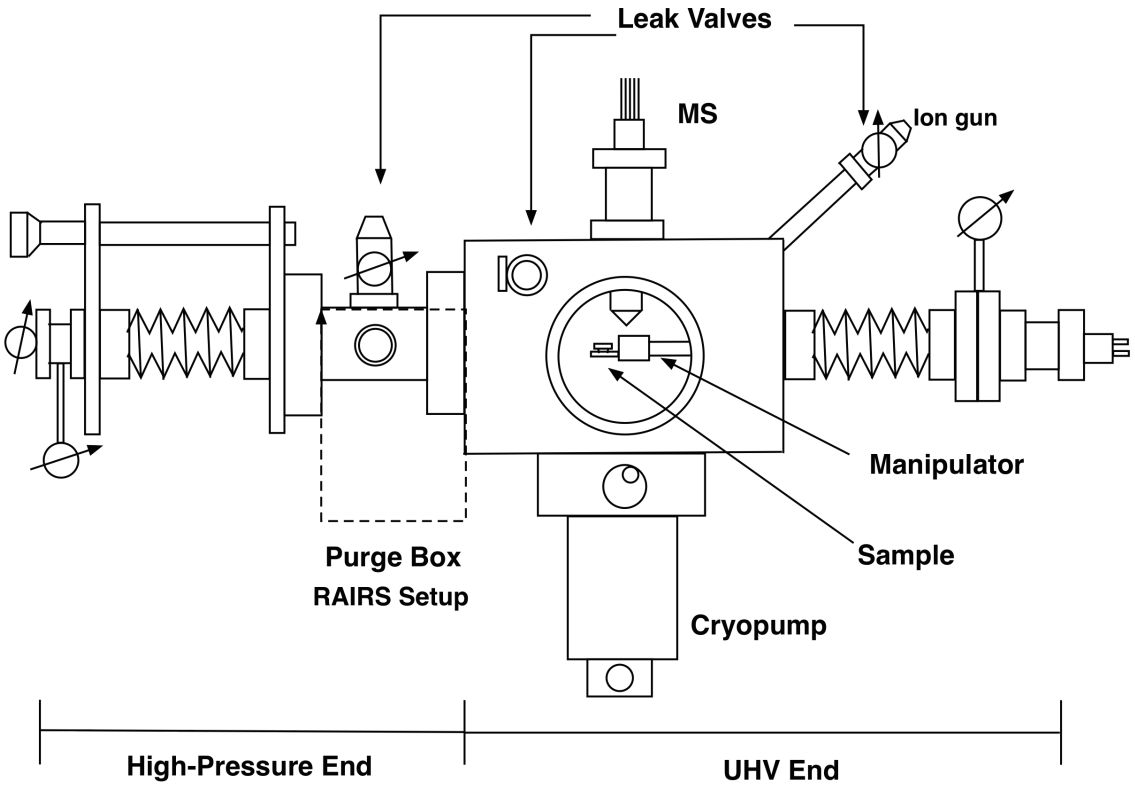

Figure 2.1. Ultra High Vacuum chamber used throughout this work. Left: High-pressure end where the High Pressure Cell is located and catalytic experiments are carried out. Right: UHV end used for cleaning the Pt (111) sample, dosing gases to cover the surface and Temperature Programmed Desorption analysis.

passed through another NaCl window and focused, with a parabolic mirror, onto a Mercury-Cadmium-Telluride (MCT) detector. The RAIRS chamber, the optics, and the detector, are completely enclosed in a sealed plastic box purged with air that has been scrubbed of water and CO_2 with a pair of Balston filters. The spectra reported in this manuscript correspond to the average of 2048 scans taken with 4 cm^{-1} resolution that have been ratioed against similarly obtained spectra of the clean sample. The second level of the UHV chamber also holds a high-pressure cell that seals with the long travel manipulator. In this way, it allows the sample to be isolated from the vacuum so it can be exposed to gas mixtures at atmospheric or near atmospheric pressures without loosing the UHV environment. With this arrangement the sample can be transferred from vacuum to catalytic conditions without exposure to outside air, probed with RAIRS during reaction and, due to a small leak from the cell to the vacuum chamber, the gases produced during the catalytic process were analyzed with mass spectrometry.

The HPC we are using presently is a new model developed by me in conjunction with Stan Sheldon, a technician that helps our group, and our machine shop, and will therefore be described in more detail here. It consists of a stainless-steel volume with a rectangular outer shape and a cylindrical inner volume of approximately 25 mL. The rectangular outer shape is bore through by two circular apertures on opposite sides where two NaCl windows are pressed by screws on two Viton O-rings, sealing the cell from any leaks. As mentioned before, the HPC is closed by coupling it with the manipulator controlled manually by the user. In order for both ends to seal, a small cylindrical cell has

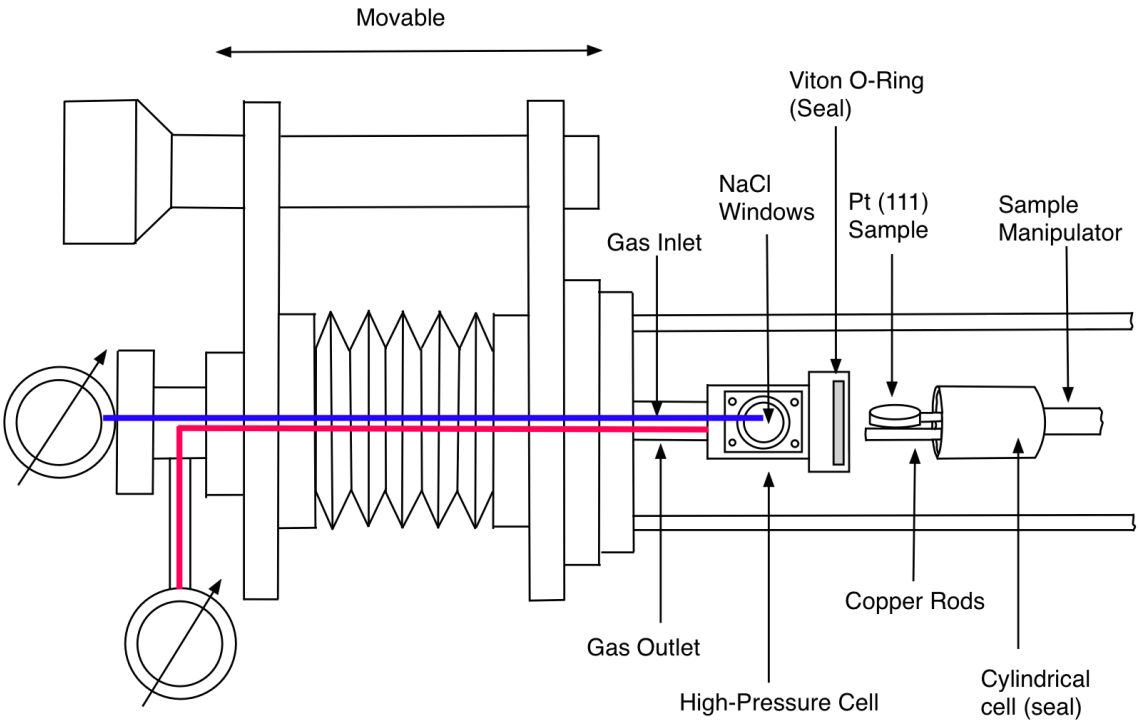

Figure 2.2. Diagram of the second deck of the Ultra High Vacuum chamber containing the high-pressure cell (HPC). The blue line represents the 1/8 in (in) gas inlet while the red line represents the gas outlet.

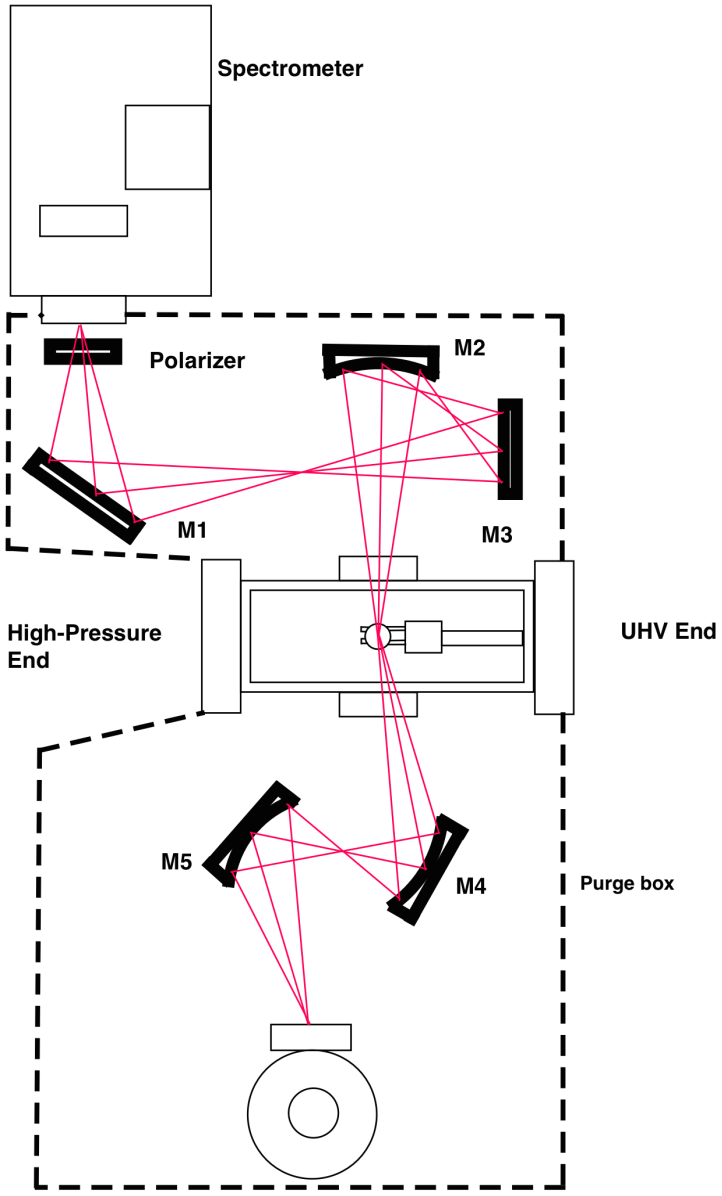

Figure 2.3. Schematic representation of the setup for RAIRS analysis. M2, M4 and M5 are parabolic mirrors used to focus the IR beam. M1 and M2 are flat mirrors used to redirect the beam to the right angles.

been placed on the feedthrough that holds the metal crystal. This cylindrical cell presses against a Viton O-ring that is wedged in a groove located in the edge of the inner volume of the HP cell.

2.3.1. Stagnant batch reactor.

A ½ in. (i.d) stainless-steel tube was connected to the opposite end of the HPC with an external manifold that was isolated from the UHV environment by a one-way Swagelok bellows valve. This manifold was connected to a MKS Baratron gauge with a reading pressure range of 0.1 -1000 Torr which was used to measure pressures for the preparation of the gas mixture. It also kept track of any pressure changes that occurred inside the cell during reaction. An adjacent 150 ml stainless-steel volume was attached to the manifold and separated with a Swagelok bellows valve that was mainly used as a reservoir for adding gas mixtures in the moment the reaction was taking place, as well as for preparing diluted gas mixtures.

2.3.2. Well-stirred batch reactor (modification of the stagnant batch reactor).

The same ½ in (i.d) stainless-steel tube from the stagnant reactor connects the opposite end of the HP cell to an external HP circulation loop that is isolated from the UHV environment by two Swagelok bellows valves that are opened when the high – pressure gases are introduced. Through this line runs a 1/8 in. (i.d) tube that is used to feed the high-pressure gas mixture into the cell. The end of this coaxial feeding line is aligned directly on top of the metal crystal. During reaction, gases are circulated through the loop by means of a Metal Bellows MB-21 stainless steel bellows-pump (BP) that allows airflow of 6 L/min. This circulation loop was fitted with the MKS Baratron gauge

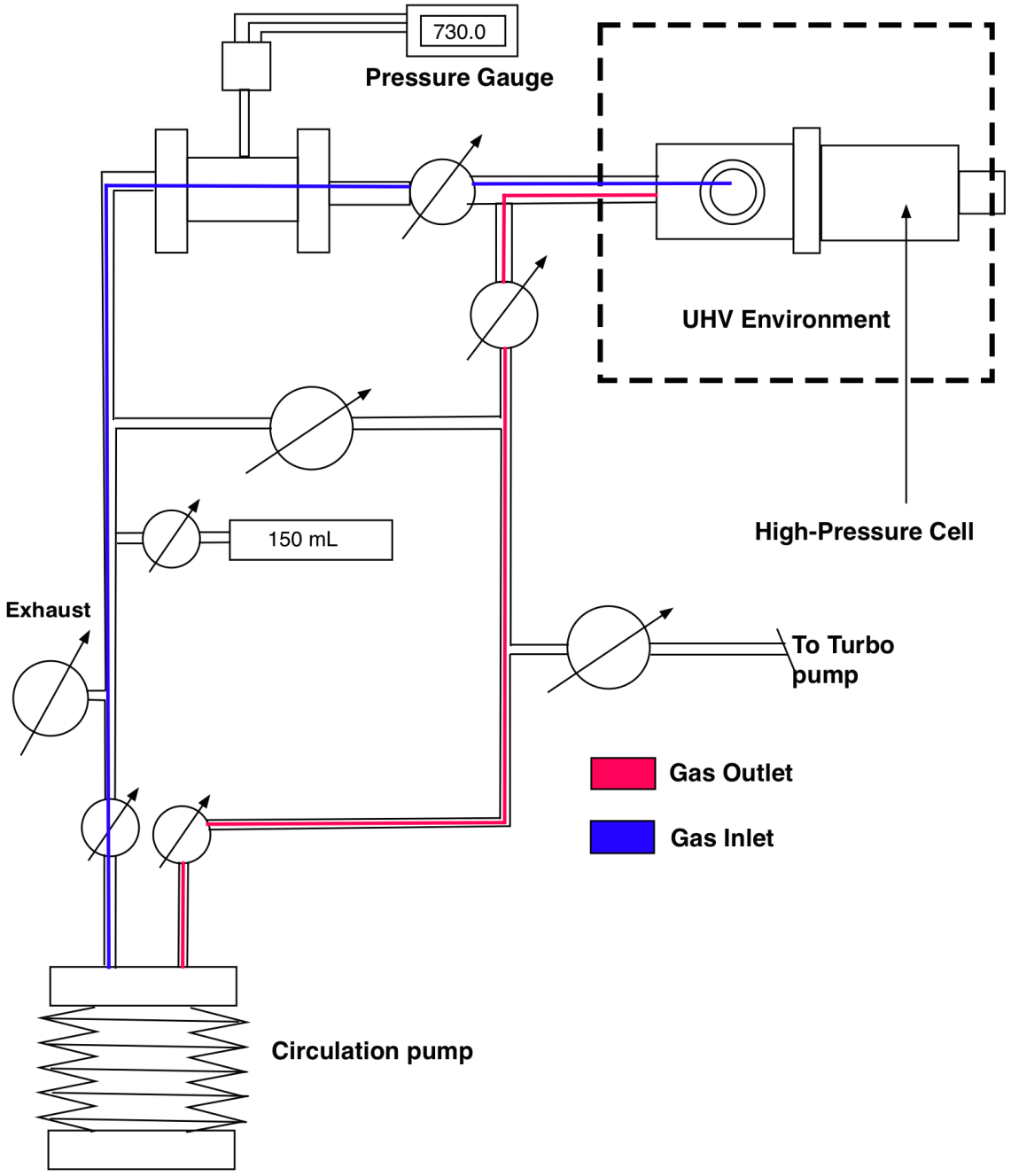

Figure 2.4. Schematic representation of the circulation loop described in section 2.3.2. The high-pressure cell is showed coupled to the sample manipulator. In this position the reactor is sealed and gasses can be circulated.

and with the adjacent 150 mL stainless steel volume from the stagnant batch reactor. Both parts carried out the same functions as in they did in the previous reactor. The HPC, the external loop, and the BP, constitute a well-mixed batch reactor. With the exception of some experiments in chapter 4 and the experiments in chapter 6, all experiments in this work were performed in the well-stirred batch reactor.

The setups described above allowed pressures between 700-760 Torr to be reached inside the cell. This pressure range causes an increase in vacuum pressure in the main UHV chamber from 10^{-10} to 10^{-5} Torr. Due in part to this fact, the cell is pumped down after each reaction using a 50 L/s Pfeiffer turbo molecular pump, to keep a pressure below 10^{-6} Torr in that side of the chamber. The pump is also necessary to reach low pressures before opening the cell to the UHV, so a sudden increase in pressure can be avoided.

2.3.3. Instrumental limitations of the reactor, manifold and circulation loop.

The stagnant reactor described in section 2.3.1 was modified due to its lack of mixing capabilities. When more than two gases were used, the MS kinetic traces showed evidence of heterogeneity in the mixture -mainly in the form of long signal delays. Also, the kinetics of H-D exchange that will be shown and discussed in chapter 5 could not be attained with this setup. The signal for HD accumulation showed a final intensity comparable to that of ethane even though hydrogen or deuterium were added in a ~ 12 times excess.

All gases were introduced by opening and closing valves by hand, which entitled an operational error. This error was significantly enhanced when gas mixtures had to be

diluted to reach olefin pressures in the mTorr range. Gas dilutions also involved acquiring aliquots of gas mixtures by partly pumping the circulation loop mechanically. This also increased the error associated to mixture preparation. This issue could not be avoided, and only limited data could be collected from experiments that used diluted gas mixtures. The best results are displayed in chapter 6.

A general limitation of the high-pressure cell is that its location and design made it hard to pump down efficiently through its small orifices and crevices, allowing for the accumulation of contaminants such as residual hydrocarbons from previous reactions, or gas dosing. This contamination was aggravated when the HPC was evacuated after each reaction, which thwarted our attempts at performing re-start reactions.

Regardless of these limitations, suitable alternatives were found or designed to work around them, enabling the acquisition of the best experimental results possible.

2.4. Surface Analysis Techniques and General Procedures.

2.4.1. Infrared Absorption Spectroscopy.

Infrared absorption spectroscopy has been widely implemented in the fields of catalysis and surface science because it is a concise and versatile technique that has enabled the identification and study of surface-bound species [3]. In addition, with the use of probe molecules like CO and NO, it has provided information regarding the number and type of active sites that are present on the surface of a catalyst [4].

The infrared spectrum spans from 10 to 10000 cm^{-1} and is divided into far infrared (10-200 cm^{-1}), mid infrared (200-400 cm^{-1}), and near infrared (4000-10000 cm^{-}

[1]). The region of most relevance in surface science is the mid-infrared, since the molecular vibrations of chemisorbed species are detected in that frequency range. The absorption of photons with frequency ν in the mid infrared range by the adsorbed species results in transitions in the discrete vibrational levels that those molecules possess. The study of the absorption frequencies that can be identified from chemisorbed molecules can yield information regarding the identity of those species, the geometry of adsorbed species, the strength of adsorption, and the nature of their bonding to the surface [5].

As mentioned above, the UHV system used in this work is setup up to carry out Reflection-Adsorption Infrared Spectroscopy (RAIRS). This technique measures the adsorption of infrared radiation due to the excitation of vibrations of surface-bound species after it is reflected from a plane substrate, usually a metal, as shown in Figure 2.5. The electric field of the incident radiation exerts a force on the effective ionic charge (e^*) of the vibrating dipole of the adsorbate, causing a loss of energy in the incident light, which results in the absorption spectrum [6].

The absorption of infrared radiation by chemisorbed molecules on the surface of a metal is markedly enhanced at higher angles of incidence (with respect to the surface normal), and it's effectively limited to p-polarized radiation [7]. Upon reflection at a given angle, the incident light beam undergoes changes in its amplitude and phase. These changes depend on the direction of the electric field (E) of the radiation. If the E is normal to the plane of incidence (s-polarized), then the resulting components of the reflected beam will be reversed in phase. And if the reflection coefficient of the material is close to unity, the resultant of the incident and reflected vectors is close to zero.

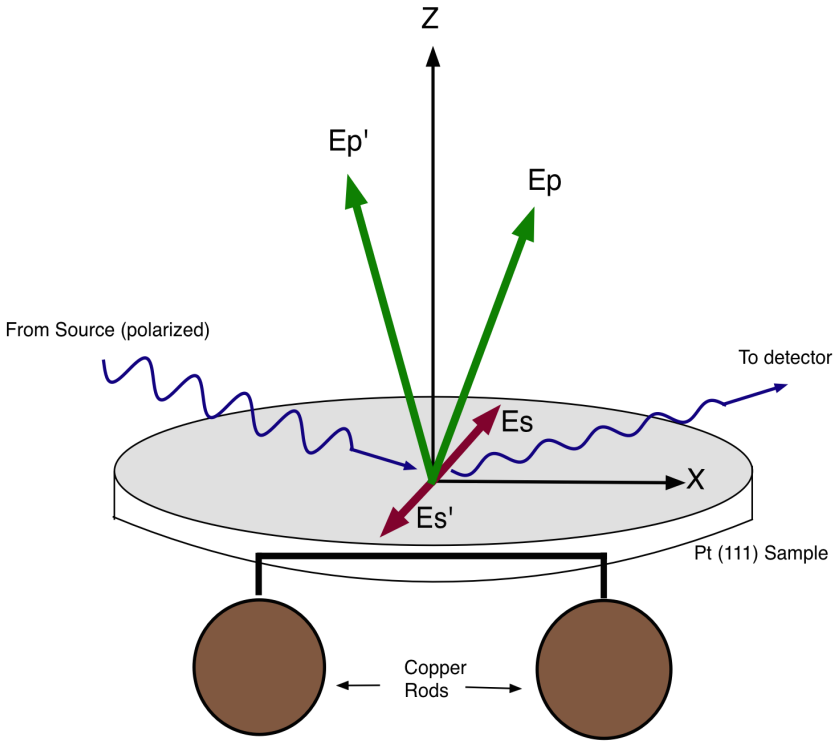

Figure 2.5. Principle of the RAIRS technique illustrated over the reflective Pt (111) sample used in the experimental setup of this work.

So s-polarized radiation cannot interact with surface dipoles. On the other hand, if the *E* of the radiation is parallel to the incident plane (p-polarized), it will suffer a phase change that depends on the angle at which the beam comes in contact with the surface. At grazing incidence the p-polarized radiation yields an almost doubly enhanced electric vector that is perpendicular to the surface ($E_{p\perp}$) and a weaker tangential vector ($E_{p||}$). Thus, p-polarized light can interact with chemisorbed molecules that have dynamic dipoles that are perpendicular to the surface, giving rise to the so-called surface selection rule [7].

Owing to its resolution (~4 cm^{-1}), the RAIRS technique has proven to be very useful in elucidating the identity of seemingly similar surface species, and with that it has aided in developing detailed molecular reaction mechanisms on surfaces. In addition, since it does not require UHV conditions for its operation, RAIRS can be employed in the *in situ* study of reactions at atmospheric or near atmospheric pressures (~700 Torr) [8], and by coupling it with a technique capable of following the chemical kinetics of the process (such as mass spectrometry), it can be used to carry out experiments under *operando* conditions [9]. An issue that arises from IR analysis of high-pressure catalytic systems is the difficulty in distinguishing between adsorbed and gas-phase species, a problem that, due to the surface selection rule, can be solved with RAIRS by simply subtracting the *s* polarized spectra from those taken for the same surface using *p* polarized light [9].

2.5. References.

[1] D. Chrysostomou and F. Zaera, *J. Phys. Chem. B*, **2001**, *105*,1003.

[2] Lee, I. and Zaera, F., *J. Phys. Chem. B*, **2005**, *1059*, 2745.

[3] Zaera, F., *Chem. Soc. Rev.*, **2014**, *43*, 7624-7663.

[4] A.V. Kiselev and V.I. Lygin, in: Infrared Spectroscopy of Adsorbed Species, L.H. Little (Ed.). Academic Press, New York, 1966.

[5] R. G. Greenler, *J. Chem. Phys.* **1966**, *44*, 310.

[6] J.W. Niemantsverdriet, *Spectroscopy in Catalysis: An Introduction*, Wiley-VCH, Weinheim, **2007**.

[7] Woodroof, D.P.; Delchar, T.A., *Modern Techniques of Surface Science Second Edition*, Cambridge University Press, **2003**, p. 356.

[8] Ohtani T.; Kubota, J.; Kondo, J.N.; Hirose, C. and Domen, J., *J. Phys. Chem. B*, **1999**, 103, 4562.

[9] Tillekaratne, A.; Simonovis, J. P.; López Fagúndez, M. F.; Ebrahimi, M.; Zaera, F., *ACS Catal.* **2012**, *2*, 2259-2268.

CHAPTER 3: GENERAL PROCEDURES. THE GENERIC HIGH-PRESSURE HYDROGENATION EXPERIMENT.

3.1 Introduction.

This chapter illustrates the general procedure followed during a routine high-pressure hydrogenation experiment. It also addresses the minor changes in experimental conditions that are used to carry out the studies shown in the following chapters. A detailed explanation of the data that is collected throughout the experiment is also offered using the hydrogenation of ethylene over an ethylidyne/ Pt (111) surface as an example.

3.2. Results and Discussion.

3.2.1. General procedure.

In general, the high-pressure hydrogenation experiment was carried out over a Pt (111) sample that was cleaned under UHV conditions with five consecutive oxidation/ annealing cycles. This clean sample was then enclosed in the HPC and exposed at 300 K to a gas mixture with a total pressure of 932 Torr that was comprised of: 2 Torr of ethylene, 50 Torr of hydrogen and 880 Torr of Ar. Argon was used as a ballast gas so the reaction could take place under atmospheric pressures (when the reaction was carried out in the stagnant reactor no ballast gas was added). The actual working pressure of the experiment was approximately 720 Torr, which was reached after the mixture was released in the HPC. During the reaction the MS kinetic traces were recorded sequentially in scans of approximately 10 minutes in duration, which allowed for the acquisition of

one IR p-polarized and one IR s-polarized spectrum per MS scan (which were later subtracted to yield the IR features of the surface species). A mass spectrum is taken at the end of the experiment to check on the distribution of products.

Minor modifications were applied to this general procedure to carry out the studies described in the subsequent chapters. These modifications are as follow:

- To study the role of strongly adsorbed hydrocarbon deposits (chapter 4) the clean sample was dosed with 40 L of either ethylene, propylene, 1-butylene, or toluene at 300 K, with the purpose of saturating the surface with an adlayer of the hydrocarbon prior to being introduced in the HPC and exposed to the reactive gas mixture.
- Probing the dissociative adsorption of hydrogen as the rate-limiting step required H-D as a reaction product for reasons that will be addressed in the introduction of chapter 5. This meant that deuterium needed to be added to the reactive gas mixture. Specifically, a mixture of 25 Torr of H_2, 25 Torr D_2, with 2 torr of ethylene topped off with 880 of Ar was used to perform these experiments.
- In Chapter 6 either 10 or 100 Torr of hydrogen were used when preparing the gas mixtures. Also, since the pressure of ethylene needed to be in the mTorr pressure regime, a 50 Torr aliquot of the prepared gas mixture was diluted with ~900 Torr of Ar. This step was repeated when further dilutions were required.

3.2.2. Example: Hydrogenation of ethylene over a Pt(111) surface saturated with an alkylidyne layer.

The evolution of the alkylidyne moieties during the catalytic reaction is followed by spectroscopic means with RAIRS. An example of the data acquired this way is shown in Figure 3.1. In this case the surface of the crystal was saturated with ethylidyne, which has a UHV spectrum on Pt (111) characterized by the following vibrational modes that have been reported elsewhere [1, 2]: the methyl symmetric stretch $\nu_s(CH_3)$ at 2882 cm^{-1}, the methyl symmetric deformation $\delta_s(CH_3)$ at 1340 cm^{-1}, and the C-C stretch ν(C-C) at 1115 cm^{-1}. The $\nu_s(CH_3)$ and $\delta_s(CH_3)$ are clearly discernable in Figure 3.1 in the spectra outside and inside the HPC. The ν(C-C) band is too weak to be observed in this particular set of spectra, but it can be identified in some cases. Given the time resolution required for the RAIRS analysis, mentioned in section 3.2, the spectra during reaction was recorded at intervals of ten minutes. After ten minutes of exposure to the reaction mixture the deformation band at 1340 cm^{-1} shows a slight shift to 1338 cm^{-1} [3] and a 42% decrease in signal intensity. However, as the reaction progressed (20 minutes) the signal shifted back to 1340 cm^{-1} and its intensity gradually decreased until it could not be discerned in the spectra taken after the HPC had been completely pumped down of the reaction gases. This effect was the result of two instrumental factors: the volume of the well-mixed batch reactor and the duration of the time resolved MS scan. These features forced the resulting ethylidyne layer to remain in contact with a hydrogen rich gas phase for approximately nine minutes after ethylene had been completely converted to ethane. This is sufficient time for the alkylidyne moieties to be hydrogenated and desorbed from

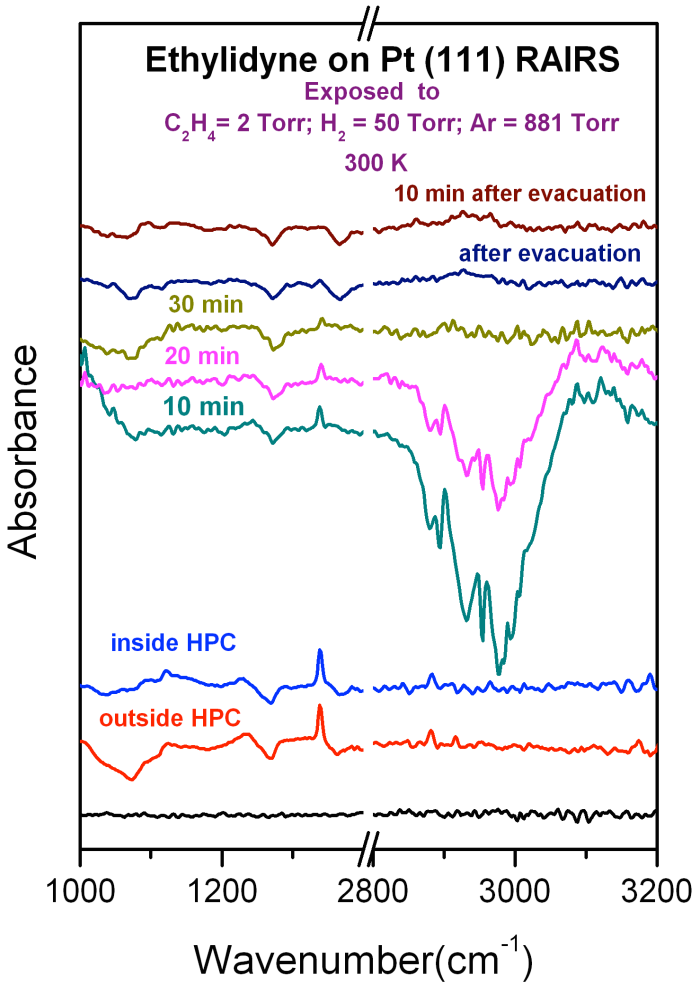

Figure 3.1. RAIRS spectra obtained before, during and after exposing an ethylidyne/ Pt (111) surface (prepared under UHV conditions) to a reaction gas mixture comprised of 2 Torr of ethylene, 50 Torr of H_2 and 880 Torr of Ar at 300 K.

the surface. Contrarily, the stagnant version of the batch reactor only requires one time resolved MS scan and its volume is much smaller, shortening reaction completion times and preventing the hydrogenation of ethylidyne after the conversion of ethylene is complete.

The spectra recorded ten and twenty minutes after exposure to the reaction gases shown in Figure 3.1 also shows a concavity in the range between 2800-3080 cm^{-1}. This spectroscopic feature is a product of the mathematical manipulation of the *p* and *s* spectra. The signal intensity of the gas phase is slightly larger in the *s*-polarized spectrum; therefore when it is subtracted from the *p*-polarized spectrum it results in a depression of the baseline. This is due to a slight mismatch caused by the high intensity of gas absorptions and the noise in the data acquisition during reaction. Thirty minutes after exposure the reaction has been completed and the *p* and *s* spectra match.

The kinetics of the catalytic hydrogenation of ethylene was followed by continuously recording the intensities of selected MS peaks that were obtained from previously reported mass spectra [4]. These peaks were chosen to best represent the species involved during reaction with the least amount of interference from all others. For this particular system, the 29 and 30 amus were used to follow the evolution of ethane because they do not show any interference from ethylene, and the 26 and 27 amus were chosen to trace ethylene after subtracting the contribution of ethane to those masses. This method is demonstrated in Figure 3.2: the left frame of the figure shows the accumulation of ethane with respect to time, represented by the linear increase of the signals for 29 and 30 amus until the reaction reaches completion at approximately 900 s. The consumption

of ethylene can also be traced but with the added difficulty of ethane interference. Only the 26 amu trace shows the evolution of ethylene throughout the reaction, since the 27 amu signal seems to cancel out due to opposite contributions from ethane and ethylene.

The ordinates of the raw data are expressed in units of signal intensity, which are arbitrary units. To express the data in chemically useful units the *y*-axis was calibrated by converting the signal intensity to pressure units (Torr), deconvoluting the raw data using MS cracking patterns first when necessary [5, 6]. Then, using the volume of the reactor and the surface area of the Pt crystal, the pressure was converted to turnover numbers (TON, molecules consumed or produced per Pt surface atom). The result of this analysis is shown in the right panel of Figure 3.2 for ethylene and ethane, using the traces for 26 and 30 amus respectively. The ethane contribution to 26 amu, along with the noise associated with the mathematical analysis carried out for unit conversion, yielded a trace with greater instrumental noise for C_2H_4 when compared with that for C_2H_6 (30 amu), making the latter more reliable for the kinetic analysis of the catalytic reaction. The near linearity -from beginning to completion- of the kinetic traces shown in the right panel of Fig. 3.2 is indicative of a pseudo-zero-order kinetics in ethylene. This pseudo-zero-order is evidence that the surface is essentially covered with ethylidyne throughout the reaction, making the turnover rate insensitive to ethylene partial pressure [7]. Under the specific conditions reported for the experiment in Fig 3.2, ethylene is completely depleted after 900 turnovers.

From the traces shown in Fig. 3.2 it is also possible to obtain the reaction rates for the consumption of ethylene and the accumulation of ethane. This is accomplished by

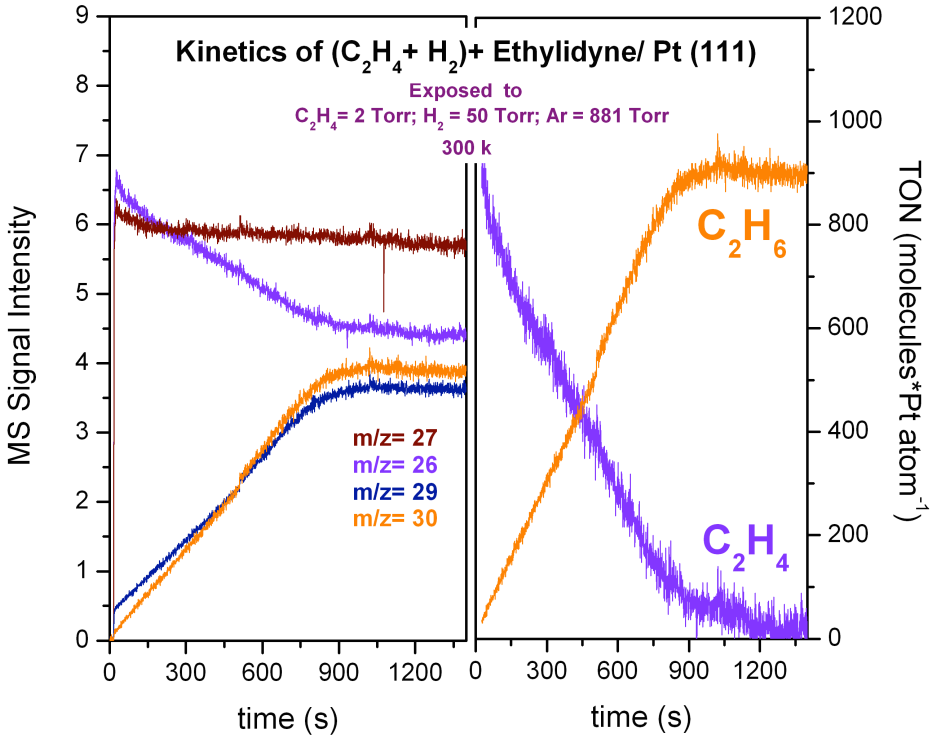

Figure 3.2. Kinetic traces obtained during the exposure of an ethylidyne-predosed Pt(111) surface (made under UHV conditions) to a reaction gas mixture comprised of 2 Torr of ethylene, 50 Torr of H_2 and 881 Torr of Ar at 300 K. Left panel: Raw data from the experiment; Right panel: Data expressed in TON (molecules consumed or produced / Pt atoms).

differentiating these traces with respect to time, which yields the corresponding turnover frequencies (TOF = TON/s), as shown in Fig. 3.3. Given that the data are acquired continuously, it is also possible to explore the time dependence of the rates, an analysis that is quite difficult to do if the kinetic data are acquired by more traditional methods as the ones reported in the literature [8, 9, 10-13]. The negative TOF values for ethylene in Fig. 3.3 correspond to its consumption during the reaction, while the positive TOF's are associated with the accumulation of ethane. Despite the noise in the ethylene trace, which has been addressed earlier, the rates seem to mirror each other up to the point where the reaction ends -within experimental error. The evolution rates of C_2H_4 and C_2H_6 seem to be constant throughout most of the catalytic reaction, confirming the pseudo-zero-order in ethylene mentioned above. In some cases a sharp spike can be noticed at some points during the rates, as is the case for the TOF's measured for ethane between 300 and 500 s. This is an experimental artifact caused by the instrumental limitation of only being able to acquire one ~ 8-minute MS scan at a time. As a consequence the recorded data shows small breaks in its continuity that are accentuated when the derivative is taken.

After the catalytic conversion of ethylene to ethane has reached completion, three consecutive mass spectra are acquired to analyze the composition of the final gas mixture. The resulting mass spectra obtained for this particular experiment are shown in Figure 3.4. Since the pressures of ethane and hydrogen differ by one order of magnitude, the signal for hydrogen (2 amu) at a MS gain set of 10^{-8} AMPS saturates and cannot be estimated. As a consequence the MS scans are taken at increasing gain set values to

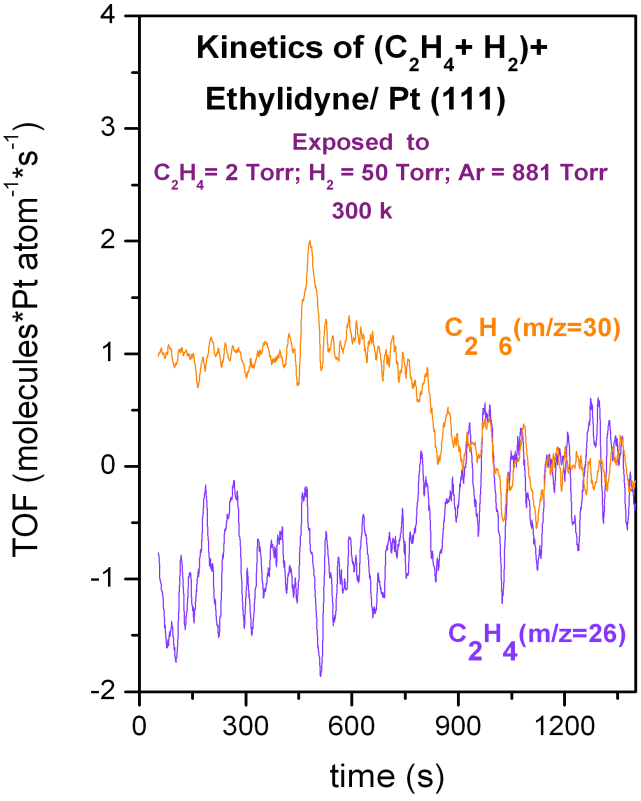

Figure 3.3. Turnover frequencies (TOF's) calculated from the kinetic traces obtained during the catalytic hydrogenation of a gas mixture comprised of 2 Torr of ethylene, 50 Torr of H_2 and 881 Torr of Ar**,** over an ethylidyne-precovered Pt(111) surface (made under UHV conditions) at 300 K.

account for every gas of interest. The signal intensity for hydrogen in particular varies very little, and a considerable excess of the gas is still observed at the end of the reaction. This is evidence that the experimental conditions at which these types of experiments are carried out are constant throughout the reaction. The spectrum at the 10^{-8} AMPS MS sensitivity setting shows that the hydrocarbon composition of the gas mixture is only due to ethane, given that the signal intensities are approximately 23, 33, 21 and 23 % of the major peak (amu 28= 100%) for the 26, 27, 29, and 30 amu values, respectively, as shown in the literature [4]. Any change in the percent of the major peaks for 26 or 27 amus might indicate the presence of unreacted ethylene, but that is not the case here. The peak intensity of 28 amu is not used because it is not reliable for the scrutiny of the hydrocarbon gas phase, since this signal includes a contribution from background CO that cannot be properly eliminated from the calculations.

The RAIRS spectra, the kinetic traces, and the mass spectra comprise the data that were routinely obtained in a typical high-pressure hydrogenation experiment. Many experiments were performed, several to check on reproducibility; the ones that show the most compelling changes will be the ones used in this work.

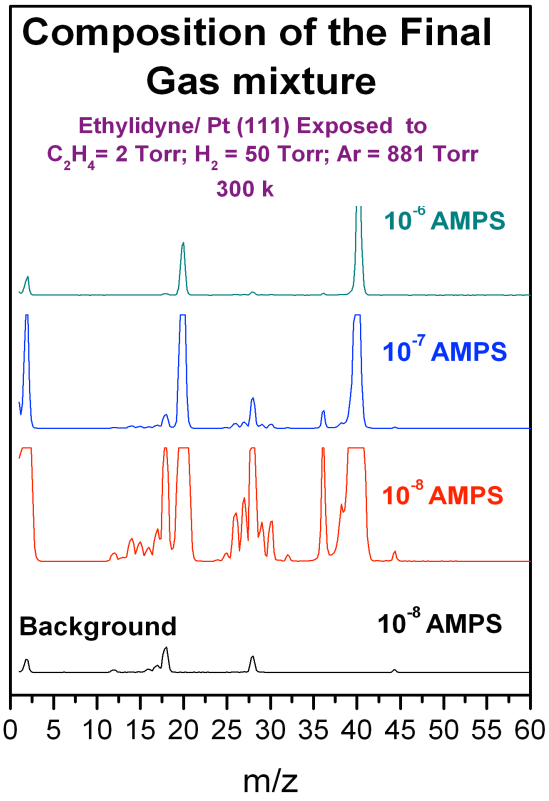

Figure 3.4. Mass spectra obtained after exposing an ethylidyne-precovered Pt(111) surface (made under UHV conditions) to a reaction gas mixture comprised of 2 Torr of ethylene, 50 Torr of H_2 and 881 Torr of Ar at 300 K.

3.3. Conclusions.

Thanks to the operando setup used in this work, it was possible to simultaneously follow the kinetics of the production of the alkane and characterize the evolution of the surface species during the catalytic hydrogenation of ethylene over Pt (111) surfaces. The results that are shown in this chapter are in good agreement with previous findings by our group and others. It was confirmed that the identity of the surface moieties is that of alkylidyne species, ethylidyne in the case of ethylene hydrogenation. The formation of ethylidyne immediately upon exposure of clean surfaces to ethylene in gas mixtures and its persistence throughout the hydrogenation of the olefin, were corroborated by the results in Fig. 3.1. Our results also show that a hydrocarbon-saturated surface can also be prepared under UHV conditions prior to the hydrogenation reaction. This is a key feature of our setup that allows us to decouple the effect of the gas phase olefin during the hydrogenation reaction as will be shown in chapter 4 of this work.

In agreement with previous findings, the gas phase kinetics of ethylene hydrogenation showed insensitivity to the changes in partial pressure of the olefin. This insensitivity is associated to the fact that the reaction is occurring over a surface that is covered with ethylidyne as evidenced in the RAIRS spectra.

The mass spectrum taken at the end of the experiment displays the complete consumption of the olefin, and also shows a negligible variation in the amount of hydrogen, which is evidence that the experimental conditions at which the reaction is taking place are constant.

3.4 References.

[1] T. V. W. Janssens and F. Zaera, *J. Phys. Chem*., **1996**, 100, 14118.

[2] Ohtani T.; Kubota, J.; Kondo, J.N.; Hirose, C. and Domen, J., *J. Phys. Chem. B*, **1999**, 103, 4562.

[3] Tillekaratne, A.; Simonovis, J. P.; López Fagúndez, M. F.; Ebrahimi, M.; Zaera, F., *ACS Catal.* **2012**, *2*, 2259-2268.

[4] P.J. Linstrom and W.G. Mallard, *NIST Chemistry WebBook*, *NIST Standard Reference Database Number 69*, **2015**.

[5] J. Wilson, H. Guo, R. Morales, E. Podgornov, I. Lee, F. Zaera, *Phys. Chem. Chem. Phys.,* **2007**, *9*, 3830-3852.

[6] J. C. F. Rodríguez-Reyes, A. V. Teplyakov, S. D. Brown, *Surf. Sci*. **2010,** *604*, 2043-2054.

[7] Cortright, R.D.; Goddard, S.A.; Rekoske, J.; Dumesid, J.A., *J. Catal.*, **1990**, *127*, 342-353.

[8] F. Zaera, G. A. Somorjai, J. Am. Chem. Soc., **1984**, *106*, 2288-2293.

[9] D. W. Blakely, E. I. Kozak, B. A. Sexton, G. A. Somorjai, J. Vac. Sci. Technol., **1976,** *13,* 1091-1096.

[10] D. W. Goodman, R. D. Kelley, T. E. Madey, J. T. Yates, Jr., *J. Catal.*, **1980**, *63,* 226- 234.

[11] C. T. Campbell, M. T. Paffett, *Surf. Sci.*, **1984**, *139,* 396-416.

[12] B. Bartlett, C. Soto, R. Wu, W. T. Tysoe, *Catal. Lett.*, **1993**, *21,* 1-10.

[13] G. H. Zhu, J. Y. Han, D. Y. Zemlyanov, F. H. Ribeiro, *J. Am. Chem. Soc*., **2004**, *126*, 9896-9897.

CHAPTER 4: THE ROLE OF THE STRONGLY BONDED HYDROCARBON DEPOSITS IN THE CATALYTIC HYDROGENATION OF ETHYLENE OVER A Pt (111) SINGLE CRYSTAL.

4.1. Introduction.

The experiments discussed in this chapter address the influence of strongly bonded hydrocarbon deposits on the rates of conversion of ethylene to ethane over a Pt (111) single crystal. These carbonaceous deposits form readily on the surface upon exposure to olefin-hydrogen gas mixtures. However, by saturating the surface of the sample with a different unsaturated hydrocarbon under UHV conditions, it was possible to decouple this effect and probe how the nature of the carbonaceous adlayer affects the rate of the Pt (111)-catalyzed hydrogenation of ethylene.

4.2. Results.

4.2.1. Displacement of alkylidyne layers by ethylidyne during ethylene hydrogenation.

The experiment shown in this section was carried out in the stagnant version of the batch reactor. Its purpose was to explore the behavior of the alkylidyne layer during the catalytic hydrogenation of olefins. In previous studies it was shown that ethylidyne could be hydrogenated under atmospheric pressures of hydrogen [1]. Moreover, a low-energy electron diffraction (LEED) analysis of the surface after hydrogenating ethylene under atmospheric pressures revealed the presence of ethylidyne [2] and *in situ* IR [3] and SFG [4] measurements have shown that this moiety is present during the reaction

confirming that the surface of the working catalysts is covered with carbonaceous deposits that result from the decomposition of the olefin in the gas phase. It has also been shown that these surface species are also hydrogenated during ethylene conversion to ethane but at a rate that is one or two orders of magnitude slower than the hydrogenation of the gas phase olefin [5].

In chapter 3 an ethylidyne layer is used to cover the surface of the single crystal before it is exposed to the reaction gas mixture. As mentioned in that section, if the HPC were to be evacuated right after the reaction is completed, the RAIRS spectrum after evacuation would show a remnant of ethylidyne. This, added to the findings from the previous studies mentioned above, suggests that the ethylidyne moieties are constantly restored by the gas phase ethylene during the catalytic reaction [6]. So, by saturating the surface of the sample under UHV conditions with another type of alkylidyne, it would be possible to decouple the effect that the gas phase has on the resulting surface species. Figure 4.1 shows RAIRS data illustrating the approach carried out in this work to test this hypothesis. Each spectrum displayed in this figure is the result of RAIRS analysis carried out 10 minutes after evacuating the gases from the HPC upon completing each run. The nine reaction cycles shown were carried out in sequence without cleaning the sample in between. The black spectrum at the bottom of the figure corresponds to an alkylidyne/ Pt(111) surface prepared under UHV conditions. The following trio of spectra correspond to the exposure of this prepared surface to three consecutive $C_2H_4 + H_2$ cycles. The resulting surface of these trials was then exposed to three consecutive cycles

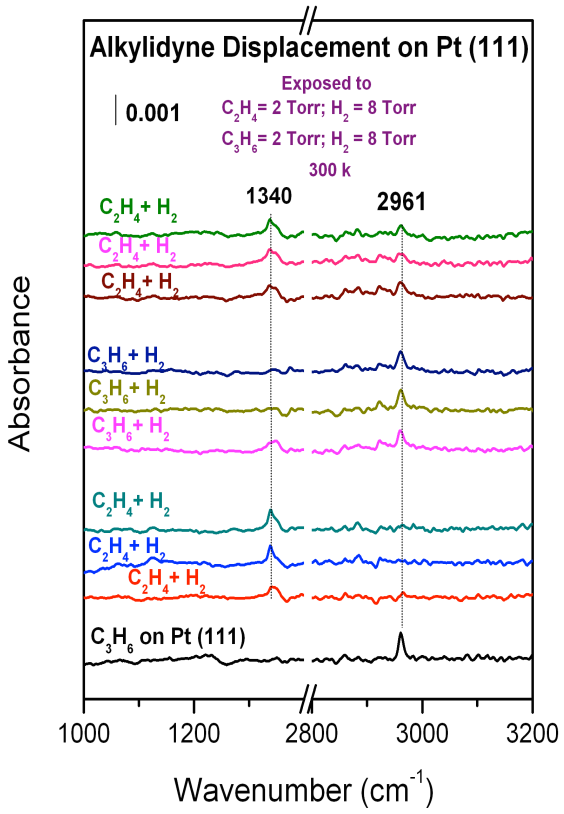

Figure 4.1. RAIRS spectra of alkylidyne-saturated surfaces taken after evacuation showing the displacement of alkylidyne layers. From bottom to top: Saturation layer of propylidyne deposited under UHV conditions (black); propylidyne-precovered Pt (111) exposed to three consecutive (2 Torr C_2H_4 + 8 Torr of H_2 at 300 K) reaction cycles (red, blue, cyan); resulting ethylidyne-saturated Pt (111) exposed to three consecutive (2 Torr C_3H_6 + 8 Torr of H_2 at 300 K) reaction cycles (magenta, dark yellow, royal blue); resulting propylidyne-saturated Pt (111) exposed to three consecutive (2 Torr C_2H_4 + 8 Torr of H_2 at 300 K) reaction cycles (wine, pink, green).

of $C_3H_6 + H_2$. Finally, the surface obtained from these runs was subjected to three back-to-back $C_2H_4 + H_2$ cycles yielding the green spectrum at the top of the figure.

For this particular experience the Pt (111) surface was first saturated with propylidyne, (the corresponding alkylidyne of propylene) in the UHV end of the chamber. The RAIRS spectrum of the resulting propylidyne is characterized by the following bands [7]: methyl rocking $\rho(CH_3)$ at 1401 cm^{-1} and 1079 cm^{-1}; C-C stretching ν(C-C) at 1104 cm^{-1}; methyl asymmetric deformation $\delta_a(CH_3)$ at 1450 cm^{-1} and its overtone $2\delta_a(CH_3)$ at 2860 cm^{-1}; methylene scissoring $\gamma(CH_2)$ at 1408 cm^{-1} and methyl symmetric $\nu_s(CH_3)$ and asymmetric $\nu_a(CH_3)$ stretchings at 2917 and 2960 cm^{-1} respectively. In Figure 4.1 the spectrum of propylidyne over Pt (111) was taken inside the HPC, which increases the signal/noise ratio even though the sample is still under vacuum conditions at that time, and therefore only the feature at 2960 cm^{-1} could be distinguished. This is the most intense feature in the propylidyne spectrum, making it the most reliable to track its evolution during reactions. After exposing the prepared surface to a 1:25 ethylene/hydrogen mixture, the $\nu_a(CH_3)$ stretching feature of propylidyne was almost absent in the spectrum after evacuation, and was replaced by the umbrella deformation mode of ethylidyne at 1340 cm^{-1}, suggesting that propylidyne is effectively displaced by ethylene to form ethylidyne. Two additional cycles of ethylene conversion completely eliminate any trace of the initial alkylidyne (propylidyne in this case) from the surface. However, the most interesting feature of Fig. 4.1 is that replacing ethylene for propylene in the gas phase actually has the same effect: three consecutive cycles of propylene hydrogenation completely displace ethylidyne from the surface and leaves only

propylidyne, implying the reversibility of the hydrogenation of the alkylidynes. Nonetheless, these changes could not easily be appreciated in the gas-phase kinetics data for this experiment.

Finally, the top three spectra in Fig. 4.1 show the persistence of the $\nu_a(CH_3)$ peak from propylidyne at 2960 cm^{-1} after the last three consecutive C_2H_4 + H_2 cycles, a shoulder on the umbrella mode from ethylidyne at 1340 cm^{-1} and a lack of smoothness on the baseline around 2960 cm^{-1}. This suggests the presence of a contaminating species from the HPC that poison the surface.

4.2.2. Kinetics of ethylene hydrogenation over propylidyne/Pt (111) surfaces vs. hydrogen pressure.

The experiments in this section were carried out in the stagnant version of the batch reactor. As in section 4.2.1, a propylidyne saturated Pt (111) surface was prepared under vacuum and exposed to an ethylene-hydrogen mixture, but in this case we varied the C_2H_4:H_2 ratio (1:25; 1:20; 1:15; 1:10; 1:5) in the initial gas mixture. The purpose of this experiment was to observe the evolution of the surface species with decreasing hydrogen pressures, and to determine if the gas phase kinetics parameters correlate with the ones reported in the literature.

Figure 4.2 shows the RAIRS spectra obtained after 10 minutes of evacuation for each experience and C_2H_4:H_2 ratio. The spectrum labeled *50 Torr of H_2* resembles the red spectrum labeled *C_2H_4 + H_2* in Fig. 4.1, since it was carried out under the same conditions. The loss in signal intensity for the asymmetric methyl stretch of propylidyne at 2960 cm^{-1} is ~ 67 % in all spectra, meaning that, regardless of the hydrogen pressure,

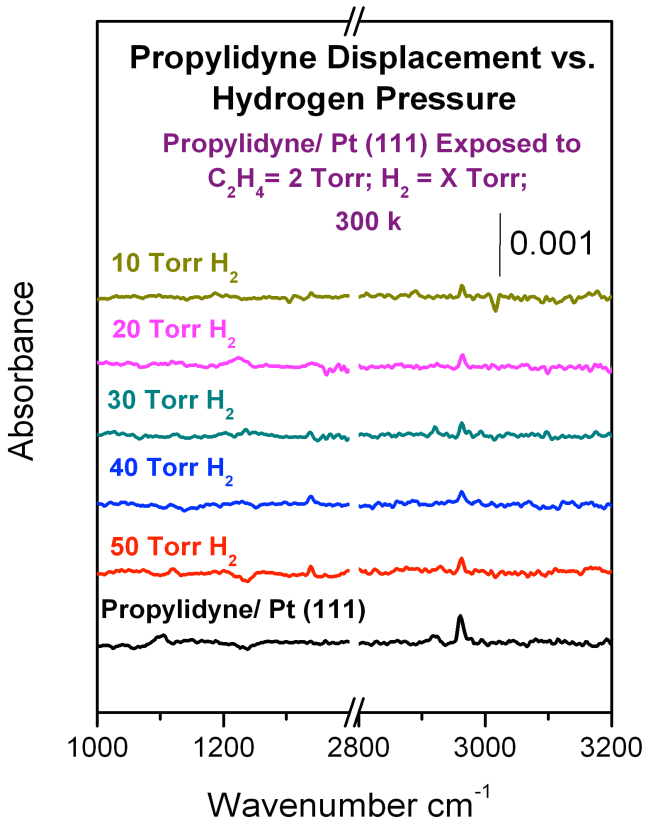

Figure 4.2. RAIRS spectra taken after evacuation showing the displacement of propylidyne with decreasing H_2 pressures.

the consumption of the propylidyne layer is approximately the same. However, with decreasing hydrogen pressures, there is a decline in the production of ethylidyne, evidenced by the weakness of its methyl umbrella mode at 1340 cm^{-1}. It seems that with higher H_2 pressures (40, 50 Torr) the rate of alkylidyne exchange over Pt (111) slows down. This behavior might be caused by the increase in co-adsorbed hydrogen coverage at high hydrogen pressures. Under these conditions such surface crowding would prevent the alkylidyne species from having enough space to undergo stepwise hydrogenation and to eventually desorb from the surface. Previous reports have shown that ethylidyne can exchange hydrogen for deuterium under UHV conditions at submonolayer coverages, indicating that this moiety can be partially hydrogenated to ethylidene on the Pt surface [8, 9]. However it is not clear if those results can be transferred to the atmospherics pressure experiments reported here.

The kinetics of ethylene hydrogenation vs. hydrogen pressure in these experiments was recorded simultaneously with our MS by tracing the changes in the 30 amu signal, as shown on Figure 4.3. As expected, the rate of conversion of ethylene to ethane, illustrated by the slope of the amu 30 traces, decreases with decreasing hydrogen pressure. In accordance with the results of section 3.2.2, the linearity of the kinetic traces of 30 amu is evidence of a pseudo-zero-order in ethelyne. Only at low H_2 pressures can a slight deviation from linearity be observed. Furthermore, a quantitative analysis of the initial reaction rates calculated from the slopes of the product traces yielded a kinetic pseudo order on hydrogen of ~1.2, which is consistent with previously reported values on Pt (111) and Pt supported catalysts [10, 11].

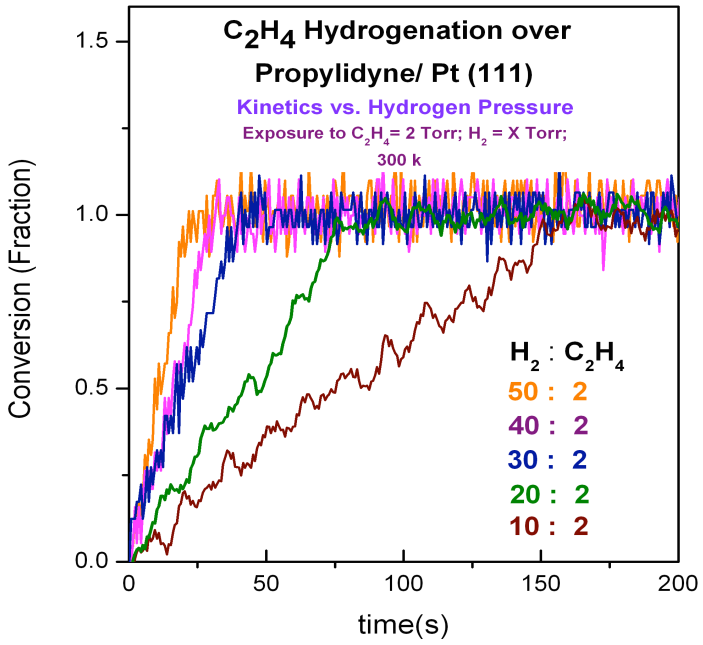

Figure 4.3. Kinetics of ethylene hydrogenation versus hydrogen pressure on propylidyne-presaturated Pt(111) surfaces. For each run, the accumulation of product is expressed in conversion fraction. Kinetic traces were obtained after exposing 2 Torr of ethylene, and X Torr of H_2 (X = 10, 20, 30, 40, 50 Torr) to a propylidyne-presaturated Pt (111) surface (prepared under UHV conditions) at 300 K.

4.2.3. Kinetics of ethylene hydrogenation vs. the pretreatment temperature of the alkylidyne layer (stagnant reactor results).

The temperature-dependent catalytic behavior of hydrocarbons chemisorbed on platinum has been studied in great detail in the past [6, 12-16]. It was found that the chemistry of these strongly adsorbed carbonaceous deposits is roughly characterized by three regimes [6]: low temperatures (<300 K), high temperatures (>750 K) and medium temperatures (~350 –750 K). The low-temperature range was characterized by the reversible adsorption of hydrocarbons and the clean metal catalysis at high hydrogen pressures. At high temperatures a multilayer carbon buildup that poisoned the surface was observed, and it hindered its catalytic properties. Finally, the mid temperature regime was marked by the richest chemistry: reversible hydrocarbon adsorption at ~ 1 atm or irreversible adsorption under UHV, with sequential bond breaking, skeletal rearrangement, and intramolecular hydrogen transfer. This range also showed catalysis by bare platinum islands in the presence of active C_xH_y fragments at high hydrogen pressures. These findings were associated to the hydrocarbon adlayer that was generated in situ from the gas-phase olefin during the catalytic reaction. The experiments carried out in this section were aimed to determine if annealing an alkylidyne layer before the catalytic hydrogenation -to form the different types of species described here- had any effects over the rate of ethylene conversion to ethane.

The experiences shown in Fig. 4.4 were done over a saturated propylidyne/Pt (111) surface that was annealed under UHV conditions to a set temperature before the hydrogenation reaction was carried out. For every trial a *fresh* propylidyne/Pt (111)

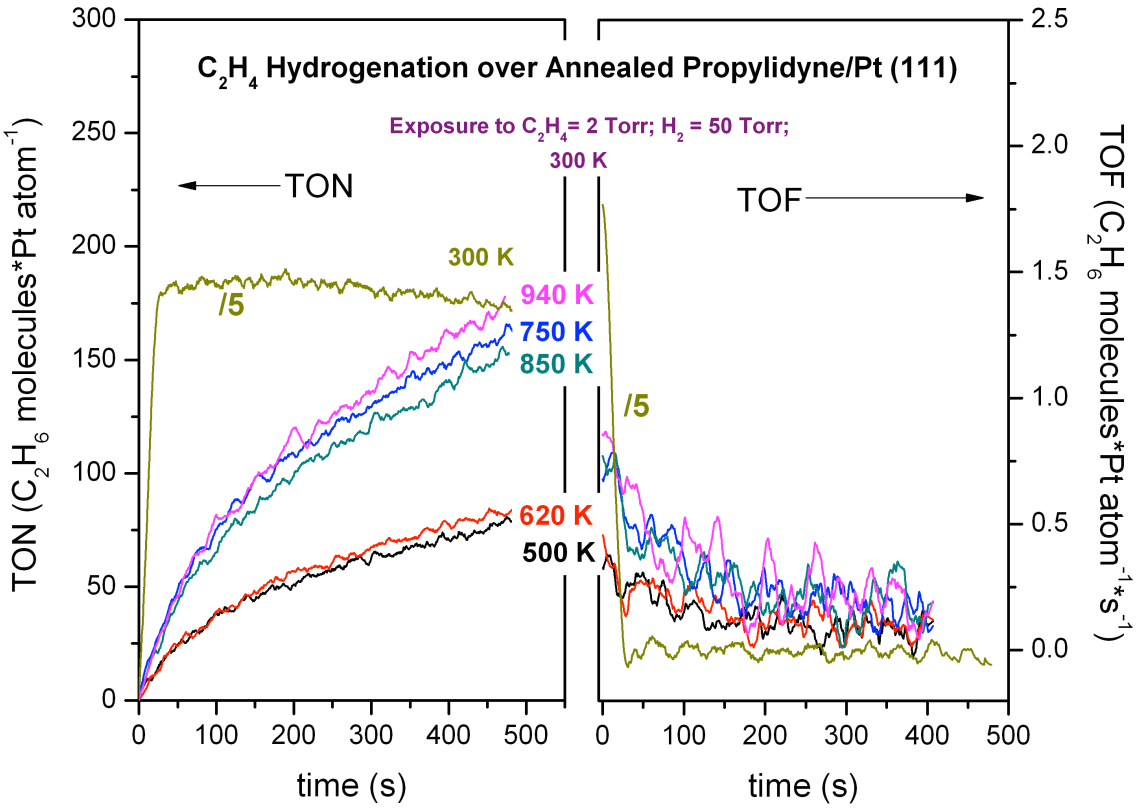

Figure 4.4. Kinetics of ethylene hydrogenation on propylidyne-pretreated Pt(111) versus the pretreatment temperature of the propylidyne adlayer. Left: Kinetics of ethane accumulation for each pretreatment temperature expressed in turnover numbers. Right: Reaction rates for each pretreatment temperature (expressed in turnover frequencies). The traces were obtained after exposing 2 Torr of ethylene, and 50 Torr of H_2 to a propylidyne-saturated Pt (111) surface (prepared under UHV conditions) at 300 K.

surface was heated to a desired temperature, meaning that each trace belongs to a sample that was prepared separately.

The left panel on figure 4.4 exhibits the traces for amu 30 (expressed in TON) after annealing each propylidyne/Pt (111) surface to the desired temperature. The panel on the right shows the reaction rates for each of these traces (expressed in TOF's). A comparison of Fig 4.4 with Fig. 3.2 shows a decrease in turnover numbers of ~ 725 ethane molecules*Pt atom between 300 and 940 K confirming that the decomposition of propylidyne at greater temperatures partially poisons the surface. However, according to the discussion on the surface species that form on the surface versus temperature regime provided earlier, no catalytic conversion should be observed above 750 K due to surface poisoning by coke. Interestingly, the reaction rates (Fig. 4.4) of surfaces pretreated at this and higher temperatures, are greater than the ones observed for those treated below 650 K, a trend that has not been reported before. This counter-intuitive behavior might be associated to the decrease in size of the pre-dosed adlayer when it is annealed under UHV conditions. Heating under vacuum conditions consumes the carbonaceous deposits, resulting in the exposure of bare Pt sites that are catalytically active as illustrated in Figure 4.5; the greater the temperature, the greater the number of exposed sites. However, this does not occur when the hydrogenation reaction is carried out at a higher temperature, since there is a continuous buildup of carbonaceous deposits due to the constant supply of the olefin from the gas phase. One feature worth noting in the left panel of Fig. 4.4 is that the ethylene conversion in the case of pre-annealing at 750 K seems to occur faster that for the 850 K case. However, the error in the measurement of

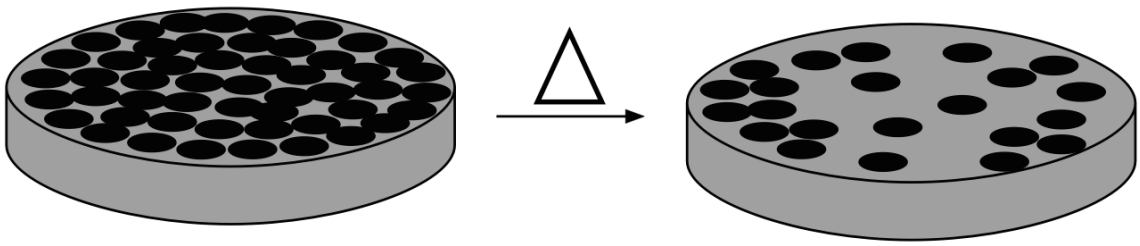

Figure 4.5. Graphical representation illustrating the shrinkage of the pre-adsorbed propylidyne layer when the surface is annealed under UHV conditions.

the gas-phase kinetics is about 10%, meaning that all of the kinetics reported here are well within the margin of our experimental error.

4.2.4. Kinetics of ethylene hydrogenation vs. the nature of the alkylidyne layer.

The hydrogenation of ethylene over Pt single crystals has been claimed to be insensitive to the structure of the metallic surface [17]. One very plausible explanation for this is that, since the surface of the working catalyst is covered with strongly bonded hydrocarbon deposits during reaction [18-22], those may smooth any structural details on the catalyst. It is therefore of importance to investigate if the nature of this hydrocarbon layer is of any consequence to the rate of conversion of ethylene to ethane. To explore the influence of the alkylidyne adlayer to the catalysis, we pre-dosed the surface of the Pt (111) crystal with unsaturated hydrocarbons of increasing molecular weight: ethylene, propylene, 1-butylene, and benzene. The C_2H_6 formation kinetics obtained from these separate trials was compared to the ethane kinetics carried out over a clean Pt (111) surface. These data are shown in figure 4.6. Except for the reaction over propylidyne/Pt (111) and toluene/Pt (111), all the traces shown in figure 4.6 are the statistical average of at least two separate trials. The error associated with these rate measurements was estimated to be ~10%, so it was safe to assume this same error for the propylidyne/Pt (111) and toluene/ Pt (111) ethane traces.

The left panel on Fig. 4.6 shows the kinetics of ethane accumulation for each trial, expressed in TON. It is clear that all the kinetics runs show linear behavior, meaning that, regardless of the nature of the hydrocarbon adlayer, the ethylene conversion is still

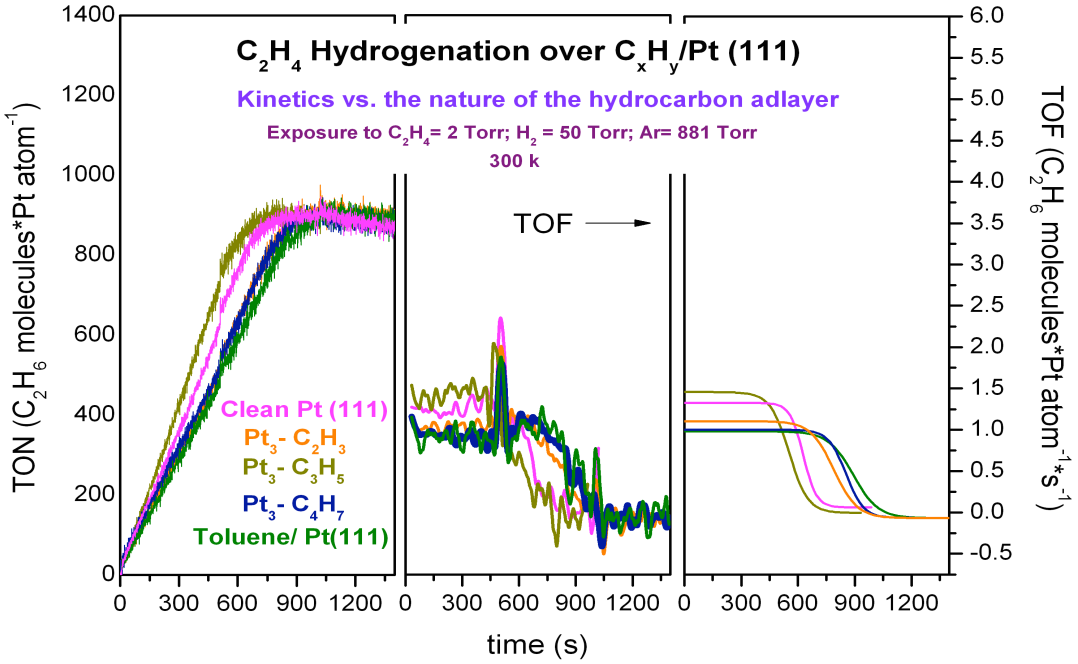

Figure 4.6. Kinetics of ethylene hydrogenation on hydrocarbon-predosed Pt(111) versus the nature of the hydrocarbon adlayer predeposited. Left: Kinetics of ethane accumulation for each C_xH_y/Pt (111) surface expressed in turnover numbers. Middle: Reaction rates for each C_xH_y/Pt (111) surface expressed in turnover frequencies. Right: Best fit of the traces shown in the middle frame. The data were obtained after exposing 2 Torr of ethylene, 50 Torr of H_2 and 881 Torr of Ar to an alkylidyne-saturated surface (prepared under UHV conditions) at 300 K.

pseudo zero order in the olefin. However, with the exception of the reaction over the propylidyne layer, it is observed that, as the molecular weight of the hydrocarbon on the surface increases, the reaction completion times become longer, indicating slower rates. This finding is supported by the TOF's shown in the middle frame of Fig 4.6. Again, note that the sharp peaks in the TOF's at 503 and 1006 s correspond to the unavoidable discontinuity in the data acquisition, and are to be disregarded. In addition, though, the C_2H_6 production traces from butylidyne/Pt (111) and toluene/Pt (111) exhibit an interesting feature at ~ 570 s, characterized by a slight increase in the TOF's with respect to time. This small convexity might be related to a switch in kinetics due to the displacement of the initial carbonaceous layer, meaning that the rate reverts to that of an ethylidyne/Pt (111) surface, once a certain amount of the initial hydrocarbon layer has been consumed. Regretfully this effect could not be confirmed with RAIRS.

The right panel of Fig. 4.6 shows the best curve fit to a sigmoidal function carried out for the ethane traces displayed in the middle frame of Fig. 4.6. The purpose of this plot is to show a clearer view TOF's vs. time. These fits cancel out the slight subtleties in the data such as the small increase in rates addressed above, but allow for the numerical estimation of the rates for each alkylidyne/Pt (111) surface. The resulting rates obtained from these fits are reported with their errors in Figure 4.7. In this figure it is easily appreciated that the propylidyne/Pt (111) surface showed the fastest conversion of ethylene to ethane. This behavior was systematically observed when the kinetics of the hydrogenation on the propylidyne-pretreated surface was compared to that on the

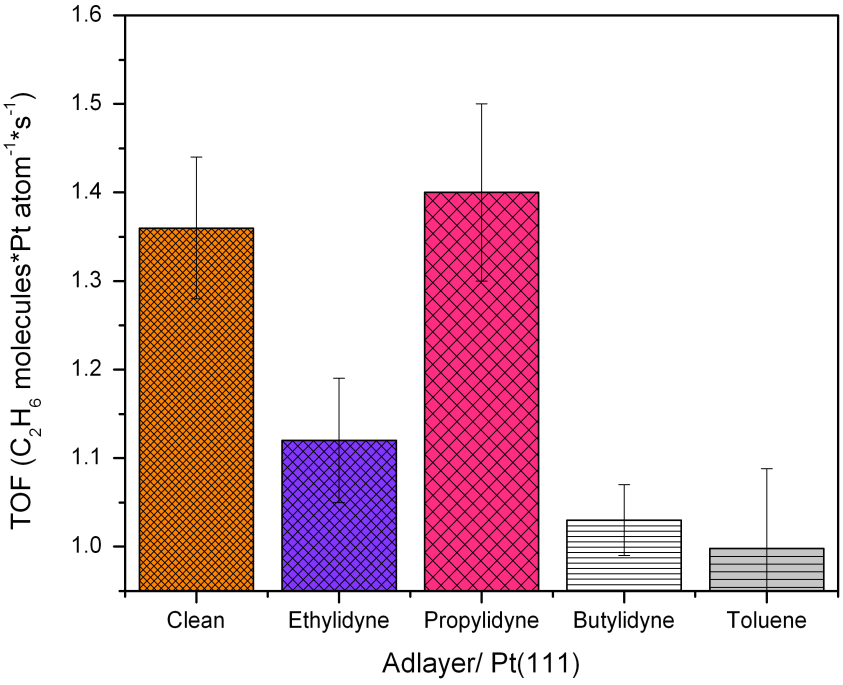

Figure 4.7. Comparison of ethylene hydrogenation rates (expressed in turn over frequencies) of Pt (111) covered with different hydrocarbon adlayers. The rates calculated from the fits shown in Fig. 4.6 are expressed with their corresponding error bars. An error of 10% was assumed for the rates calculated from the experiments over a propylidyne and toluene adlayer since all other measurements showed a deviation close to the value.

ethylidyne/Pt (111) case. Unexpectedly, the kinetics on the propylidyne-predosed Pt (111) surface is also comparable to that measured on clean Pt (111). RAIRS studies of propylidyne on Pt (111) have shown that its surface configuration depends on coverage [7]: on a surface that is saturated with this species the terminal methyl is tilted with respect to the surface normal. However at lower coverages the same methyl moiety lies flat on the surface in accordance with the surface selection rule on metals [23]. As shown in Fig. 4.1 and 4.2, the coverage of propylidyne decreases during the hydrogenation reaction. This decrease might be enough to ensure a change in the surface configuration of the alkylidyne making it less of a physical hindrance than the other hydrocarbons for the hydrogenation of ethylene. However, with the current results, it is difficult to support this claim.

4.3. Discussion.

The spectra from Figs. 4.1and 4.2 show evidence for the hydrogenation of the strongly adsorbed carbonaceous deposits under the conditions of olefin hydrogenation reaction, but at a much slower rate than the turnover frequencies of gas-phase ethylene to ethane. In particular, Fig. 4.1 shows that the alkylidyne layer can be readily displaced by the olefin in the gas mixture, suggesting reversibility in the rates of hydrogenation when olefins are alternated. However, due to the limitations of the HPC setup, this direction of research could not be explored further. Nonetheless, these findings are consistent with previous studies of the removal of alkylidynes using ex-situ vibrational spectroscopy and deuterium labeling [24, 25].

Additionally a new and unexpected behavior was discovered regarding the rate at which slkylidynes are exchanged on the Pt (111) surface. It seems that this rate is slower at greater hydrogen pressures (40, 50 Torr), a trend that might be related to the lack of reactivity of these species due to surface crowding by hydrogen atoms at these high pressures. It is worth noting that regardless of this behavior the olefin in the gas phase was still hydrogenated at a faster rate with increasing hydrogen pressures.

A new and counter-intuitive finding of this work was that by increasing the annealing temperature at which a previously prepared propylidyne-presaturated Pt (111) surface is subjected to, the rate of ethylene conversion to ethane increases. The expectation is that, after higher annealing temperatures, the hydrocarbon layer would decompose into graphite [6], poisoning the surface and hindering its catalytic activity. It would seem that without the constant supply of the olefin during sample heating, propylidyne is progressively dehydrogenated to more stable and site blocking species, all the way to graphitic deposits, but that in the process some of the carbon may desorb and the rest compact on the surface, blocking a smaller fraction. This shrinkage of the adlayer may lead to the opening of bare Pt sites, which then become available for the catalytic process.

A new idea explored in this work was the possible dependence of ethylene hydrogenation rates on the nature of the pre-adsorbed hydrocarbon layer. Preparing a Pt (111) surface saturated with strongly adsorbed hydrocarbon deposits before carrying out the catalytic process, enabled us to decouple the formation of that layer from the olefin hydrogenation reaction. Fig. 4.6 shows that this decoupling effect is real but perhaps

short lived, since the pre-adsorbed alkylidyne is readily displaced by the corresponding alkylidyne that may form from reaction of the olefin in the gas phase with the surface. Nonetheless, its initial presence seems to affect the rate of reaction, as can be appreciated in the TOF's values shown in Fig. 4.7. In general, the assumption that carbonaceous deposits with greater molecular weight will decrease the reaction rates due to surface site blocking, holds for most of the unsaturated hydrocarbons tried in this work, with the notable exception of propylidyne.

4.4. Conclusions.

The catalytic hydrogenation of ethylene over Pt (111) showed fast conversion rates and kinetic parameters in accordance to those reported previously in the open literature. In addition, the formation and persistence of the alkylidyne layer that forms readily on the surface upon exposure to the gas mixture was also observed. The results from this chapter help to corroborate that these alkylidyne moieties are not directly involved in the mechanism of olefin hydrogenation, since their hydrogenation occurs at a much slower rate than that of the gas phase ethylene. Their presence is a physical hindrance that prevents accessibility to catalytically active Pt sites. However, in their own kinetic regime these carbonaceous deposits posses a certain amount of mobility and reactivity, since they can be displaced over time and replaced by the alkylidyne corresponding to the olefin present in the gas phase.

New evidence of the physical obstruction of catalytically active sites by strongly adsorbed carbonaceous deposits with different structures is also reported here. Heavier

deposits were seen to, in general, slow down the catalysis more, although by a relatively small fraction. An exception to this behavior was seen with propylene, which does not seem to significantly obstruct the surface active sites.

Finally, heating a pre-dosed hydrocarbon layer under vacuum causes the dehydrogenation and fragmentation of said adsorbates and as a consequence the number of bare Pt sites available for catalytic conversion increases. Surprisingly, the ethylene hydrogenation TOF's obtained with surfaces prepared using this methodology increase with growing annealing temperatures, in spite of the upsurge in irreversibility of the layer made this way.

4.5. References.

[1] Davis, S. M.; Zaera, F.; Gordon, B. E. and Somorjai, G. A., *J. Catal.,* **1985**, *2*, 240-246.

[2] Zaera, F. and Somorjai, G.A., *J. Am. Chem. Soc*, **1984**, 106, 2288-2293.

[3] Ohtani T.; Kubota, J.; Kondo, J.N.; Hirose, C. and Domen, J., *J. Phys. Chem. B*, **1999**, 103, 4562.

[4] Cremer, P. S.; Su, X.; Shen, Y. R.; Somorjai, G. A., *J. Am. Chem. Soc.* **1996**, *118*, 2942-2949.

[5] Tillekaratne, A.; Simonovis, J. P.; López Fagúndez, M. F.; Ebrahimi, M.; Zaera, F., *ACS Catal.* **2012**, *2*, 2259-2268.

[6] Davis, S.M.; Zaera, F. and Somorjai, G.A., *J. Catal.*, **1982**, 439-459.

[7] Zaera, F. and Chrysostomou, D. *Surf. Sci.* **2000**, *457*, 71.

[8] Koel, B. E.; Bent, B. E.; Somorjai, G. A., *Surf. Sci.* **1984**, *146*, 211.

[9] Janssens, T. V. W.; Stone, D.; Hemminger, J. C.; Zaera, F. *J. Catal.,* **1998**, *177*, 284.

[10] D. W. Goodman, R. D. Kelley, T. E. Madey, J. T. Yates, Jr., *J. Catal.*, **1980**, *63,* 226- 234.

[11] Horiuti, J.; Miyahara, K. Hydrogenation of Ethylene on Metallic Catalysts; NSRDS-NBC No. 13; National Bureau of Standards: Washington, DC, **1968.**

[12] Gillespie, W. D.; Herz, R. K.; Petersen, E. E.; Somorjai, G. A., *J. Catal.*, **1981**, *70*, 147.

[13] Herz, R. K., Gillespie, W. D., Petersen, E. E., and Somorjai, G. A., J. Catal., **1981**, 67, 371.

[14] Smith, C. E.; Biberian, J. P.; Somotjai, G. A., *J. Catal*., **1979**, *57*, 426.

[15] Blakely, D. W., and Somorjai, G. A., *J. Catal*., **1976**, 42,181.

[16] Davis, S. M. and Somorjai, G. A., *Surf. Sci*., **1980**, 91, 73.

[17] Schlatter, J. C. and Boudart, M., *J. Catal*., **1972**, 24, 482.

[18] Hattori, T., and Burwell, R. L., Jr., J. Phys. Chem., **1979**, *83*, 241.

[19] Paal, Z., Dobrovolszky, M., and Tetenyi, P., J. Catal., **1977**, *46*, 65.

[20] Lankhorst, P. P., DeJongste, H. C., and Ponec,V., in "*Catalyst Deactivation*" (B. Delmon and G. F. Foment, Eds.). Elsevier, Amsterdam, **1980**.

[21] Paal, Z., and Tetenyi, P., *J. Catal*., **1973**, *30*,350.

[22] Trimm, D. L., *Catal. Rev*.,**1977**, *16*, 155 and references cited therein.

[23] R. G. Greenler, *J. Chem. Phys.* **1966**, *44*, 310.

[24] Koel, B. E.; Bent, B. E.; Somorjai, G. A., *Surf. Sci.* **1984**, *146*, 211.

[25] Wieckowski, A.; Rosasco, S. D.; Salaita, G. N.; Hubbard, A.; Bent, B. E.; Zaera, F.; Godbey, D.; Somorjai, G. A. J. Am. Chem. Soc. **1985**, *107*, 5910.

CHAPTER 5: THE DISSOCIATIVE ADSORPTION OF HYDROGEN AS THE RATE-LIMITING STEP IN THE CATALYTIC HYDROGENATION OF ETHYLENE OVER Pt (111) SINGLE CRYSTALS.

5.1. Introduction.

As mentioned in the chapter 1, the catalytic hydrogenation of olefins over transition metals requires the presence of surface hydrogen [1], which originates from the reversible dissociative adsorption of the H_2 molecule. In addition, these reactions typically display close-to-first-order kinetics with respect to hydrogen, suggesting that its dissociation on the surface might be the rate-limiting step [1]. Taking advantage of the reversibility of this step and using deuterium isotope labeling, it was possible to follow the formation of H-D (3 amu) from the isotope scrambling that occurs on the surface while the catalytic hydrogenation of ethylene with H_2+D_2 mixtures takes place. The production of HD is directly correlated to the dissociation of the H_2 and D_2 on the metal surface, and can be used as evidence to probe the role of this step in the hydrogenation mechanism. The results from this chapter revealed that the H-D scrambling followed non-linear kinetics under the particular reaction conditions used in this work, an unexpected and undocumented behavior.

5.2. Results.

5.2.1. Hydrogenation of ethylene over a Pt (111) single crystal with a 1:1 H_2/D_2 gas mixture. The typical experiment.

Essentially all the RAIRS spectra for the experiments performed in this chapter display the same features and behavior since the olefin in question is always ethylene. An example of the RAIRS spectra collected during the hydrogenation/deuteration reaction of ethylene over Pt (111) is shown in Figure 5.1. The characteristic peak that is exhibited throughout the reaction is the methyl deformation mode $\delta_s(CH_3)$ of ethylidyne at 1340 cm^{-1} [2, 3]. This is expected, since part of the gas-phase olefin readily decomposes on the surface and yields the corresponding alkylidyne, as explained and demonstrated in Chapter 4.

The 1340 cm^{-1} peak is first observed in the spectrum 10 min after exposure to the reaction mixture. Its intensity decreases gradually, until its presence is barely noticeable 10 min after the HPC has been evacuated. The disappearance of this signal is mainly due to the prolonged exposure of the alkylidyne to the hydrogen/deuterium-rich gas phase after the catalytic hydrogenation has reached completion. It is worth noting that these surface species undergo substantial H-D exchange [4], and the absence of frequency shifts in our spectra that could be associated to this exchange reaction may be due to a instrumental sensitivity issue. Therefore the H-D exchange between ethylidyne and the gas phase deuterium cannot be ruled out.

Additionally, a broad and unidentifiable peak is often observed around 1410 - 1480 cm^{-1} only during reaction suggesting the presence of other organic moieties. This region is characteristic of C-H deformation modes, however, it is difficult to assign this band with the IR information alone [5]. Finally, a small peak at 2960 cm^{-1} is observed in the spectra recorded after evacuation, and corresponds to the methyl asymmetric $\nu_a(CH_3)$

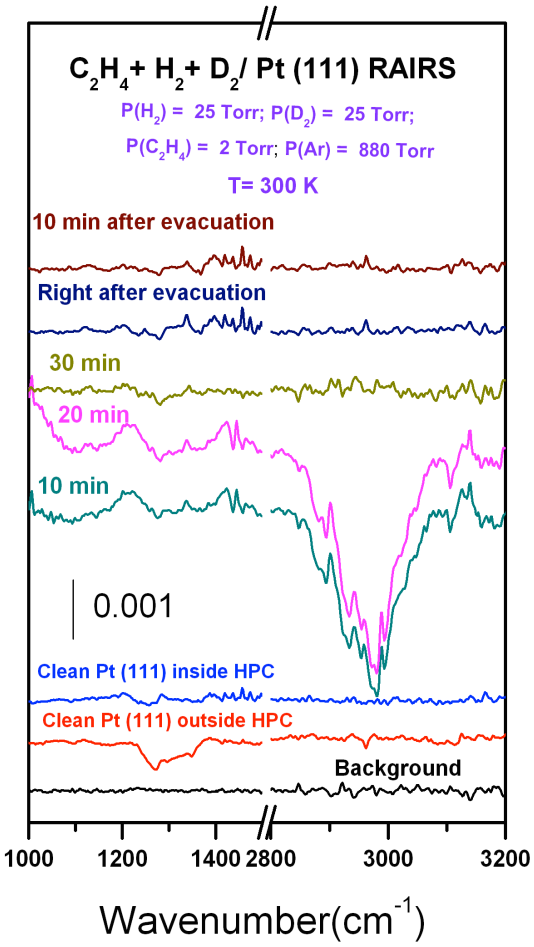

Figure 5.1. RAIRS spectra obtained before, during and after exposing a clean Pt (111) surface (prepared under UHV conditions) to a reaction gas mixture comprised of 2 Torr of ethylene, 25 Torr of H_2, 25 Torr of D_2 and 881 Torr of Ar at 300 K.

stretching mode. Its presence might be associated to the HPC contamination that is commonly aggravated after evacuation of the cell. This signal is characteristic of propylidyne on Pt (111).

Figure 5.2 shows the kinetic traces expressed in terms of TON (molecules*Pt atoms^{-1}) that were typically obtained in the experiments carried out in this chapter. They are characterized by strong signals for 3, 26, 30, 31, 32 amus and the total products (gray trace = C_2H_6 + C_2H_5D + $C_2H_4D_2$) that correspond to HD, ethylene (C_2H_4), ethane (C_2H_6), mono-deuterated ethane (C_2H_5D), di-deuterated ethane ($C_2H_4D_2$) and C_2X_6 respectively. Those species alone accounted for all the consumed ethylene, and no other deuterated species of ethane were detected, as corroborated by comparing the MS signal intensities of the total C_2X_6 trace and the initial C_2H_4 trace, which mirrored each other (within experimental error). These results are in good agreement with previously documented results with C_2H_4 + D_2 over Pt (111) surfaces, where C_2H_5D and $C_2H_4D_2$ were the statistical majority found after reaction [6].

The most intriguing feature from Figure 5.2 is the sudden switch in the kinetics of HD production at around 750 s. Even though previous studies [7, 8, 9, 10] have shown that the rate of H-D exchange in H_2 + D_2 mixtures decreases in the presence of olefins, it has never been reported (to the best of our knowledge) that the kinetics of this exchange switches in a non-linear fashion during the catalytic hydrogenation of ethylene, as seen here. The right frame of Fig. 5.2 displays the H-D exchange traces obtained over a Pt (111) surface in the presence (brown trace) and absence (blue trace) of ethylene. From this representation it is clear that the inflection in the curve that shows the kinetic switch

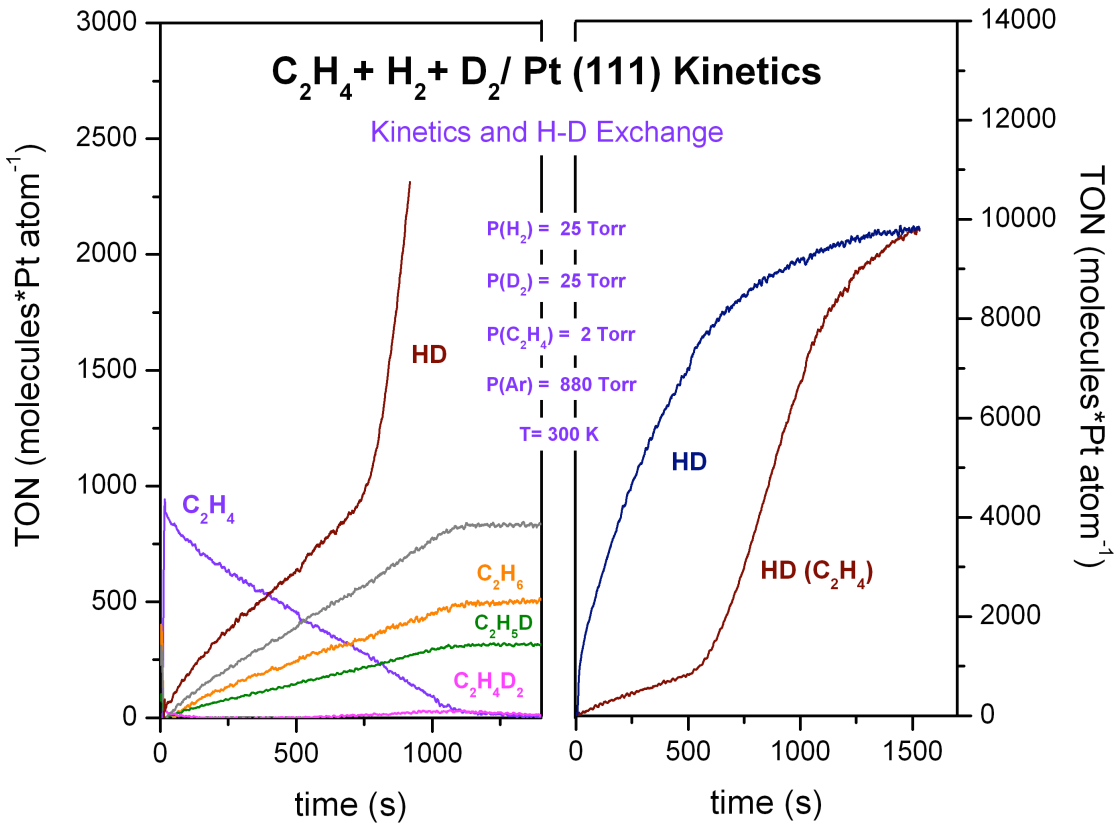

Figure 5.2. Ethylene hydrogenation kinetics and HD production after exposing a clean Pt (111) surface to a (2 Torr C_2H_4 + 25 Torr of H_2 +25 Torr of D_2 and 880 Torr of Ar) at 300 K. Left: Kinetics of ethylene hydrogenation and HD formation expressed in turnover numbers (TON). Right: HD formation in (TON) as a function of time in experiments with (HD (C_2H_4)) and without (HD) ethylene in the gas phase.

is only seen in the presence of the olefin. However, it is puzzling that this switch occurs approximately 300 s before the hydrogenation/deuteration reaction of ethylene is completed, since for this particular system (C_2H_4 + H_2/ Pt (111)) any sudden increase in the production of HD would have expected to occur right after the conversion of ethylene to ethane is complete instead. This observation suggests that the origin of this behavior is not trivial. In absence of simple explanation, the experiments carried out throughout this chapter were designed to explore the underlying causes of these phenomena.

Fig 5.3 displays the (MS) analysis of the final gas mixture. The spectrum collected at a gain value of 10^{-8} AMPS shows the peaks at 26, 30, 31, 32 amus that correspond to C_2H_4, C_2H_6, C_2H_5D, and $C_2H_4D_2$, respectively. The spectrum at 10^{-7} AMPS exhibits the statistical distribution, ~ 1: 2: 1 H_2/HD/D_2 (2/3/4 amu), expected from full scramble of the hydrogen gas according to the stoichiometry of the reaction, $H_2 + D_2 \rightarrow 2$ HD when an initial 1:1 H_2/D_2 mixture is used. Finally, at a gain value of 10^{-6} AMPS, Fig. 5.3 only shows the peaks of Ar (20 & 40 amu), the dominant gas in the reaction mixture.

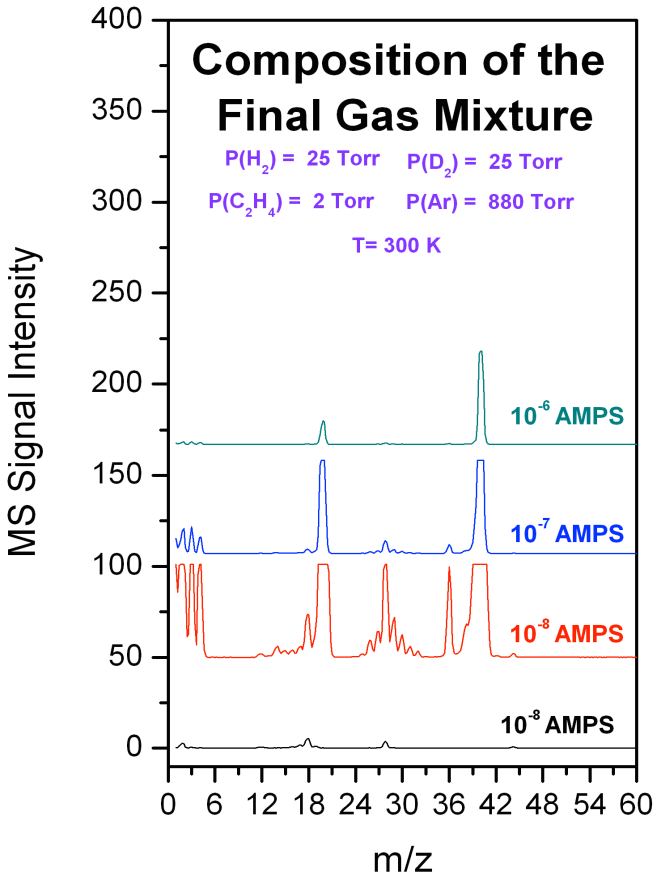

Figure 5.3. Mass spectra obtained after exposing a clean Pt (111) (prepared under UHV conditions) to a reaction gas mixture comprised of 2 Torr of ethylene, 25 Torr of H_2, 25 Torr of D_2 and 880 Torr of Ar at 300 K for 30 minutes.

5.2.2. HD kinetic trace behavior.

Since the sudden switch in the HD production trace has not been documented before, it was necessary to test its occurrence in a variety of scenarios in order to prove that its origin is not caused by experimental or instrumental artifacts. One of these test settings was already described in Fig. 5.2, where the HD exchange was carried out in the absence of the olefin to confirm that the non-linearity of its kinetics was related to the catalytic hydrogenation of ethylene over the metal surface. The next step was to alter the nature of the surface by saturating it with alkylidynes. For this purpose, $C_2H_4 + H_2 + D_2$ gas mixtures (prepared as mentioned in chapter 3) were converted separately on ethylidyne/Pt (111) and propylidyne/ Pt (111) surfaces at room temperature. The results of these trials are depicted in Figure 5.4: the left panel corresponds to the experience over a clean Pt (111) surface from Fig, 5.2, while the middle and right panels are associated to the ethylidyne- and propylidyne-covered Pt surface, respectively. According to the findings of Fig. 5.4, the general trends, including the sudden inflection in the production of HD seen toward the end of the reaction, occur regardless of the nature of the surface adlayer. However, it seems that with propylidyne the time of its occurrence increases by ~ 300 s, suggesting slower reaction rates. This behavior is opposite to the results from chapter 3 where it was found that, in the absence of deuterium, the catalytic hydrogenation of ethylene over a propylidyne/Pt (111) surface occurred at a rate comparable to that obtained with the clean Pt surface. It might be possible that the initial surface for this trial was not as clean as expected and the addition of propylene further

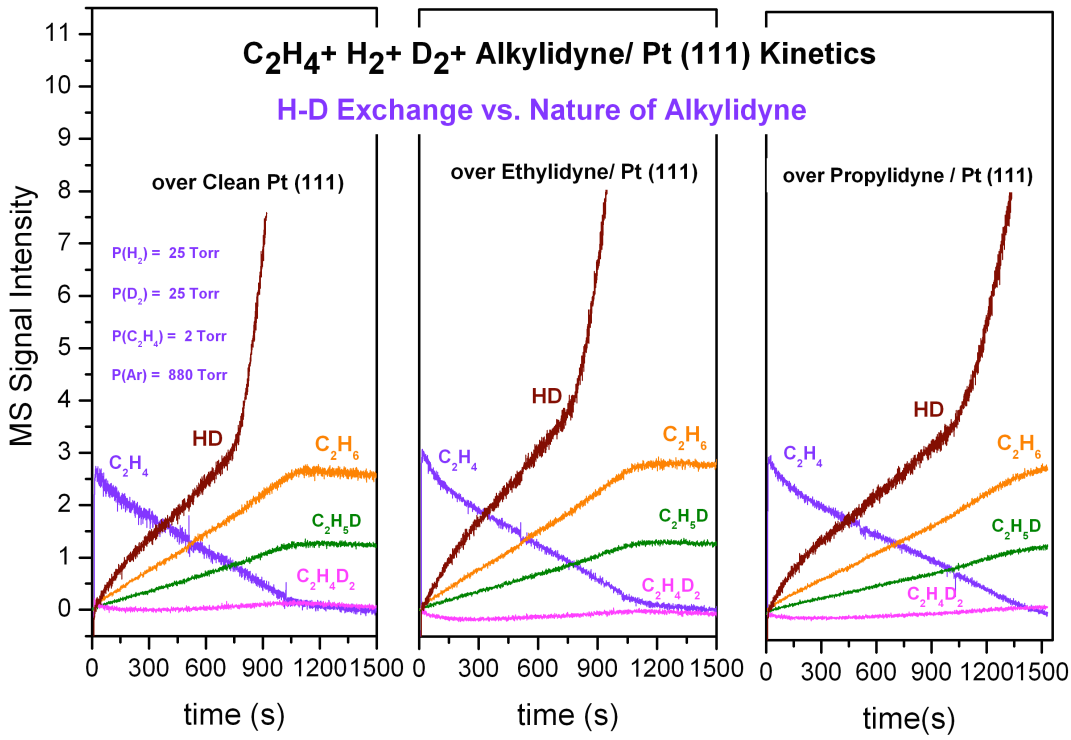

Figure 5.4. H-D exchange vs. the nature of the alkylidyne layer. Kinetics obtained after exposing surfaces to a (2 Torr C_2H_4 + 25 Torr of H_2 + 25 Torr of D_2 and 880 Torr of Ar) at 300 K. Left: H-D exchange over a clean Pt (111) surface. Middle: H-D exchange over an ethylidyne/Pt (111) surface. Right: H-D exchange over a propylidyne/Pt (111) surface.

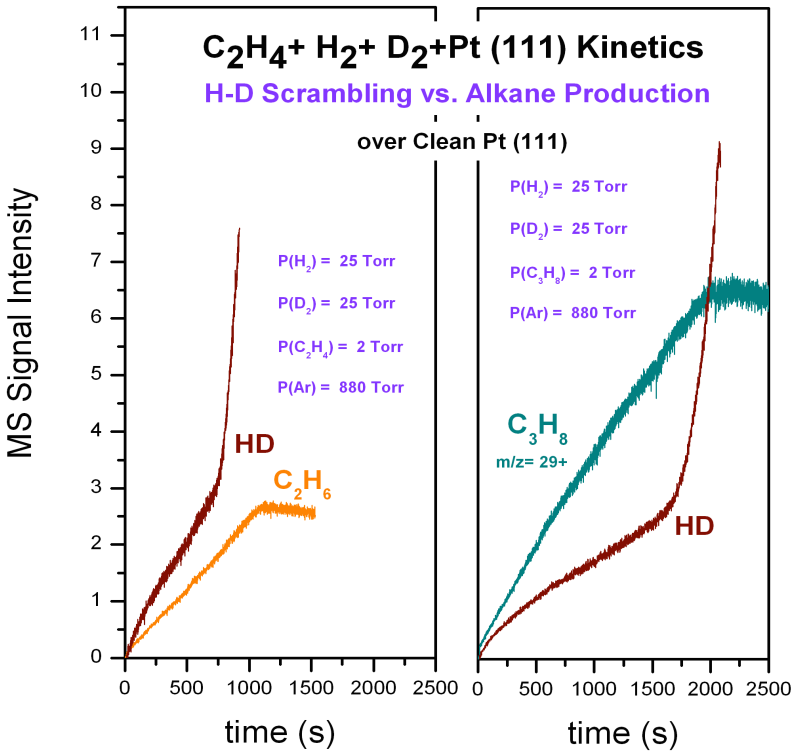

Figure 5.5. H-D vs. alkane production. Kinetics obtained after exposing a clean Pt (111) surface to a: *Left*: (2 Torr C_2H_4 + 25 Torr of H_2 +25 Torr of D_2 and 880 Torr of Ar) at 300 K. *Right*: (2 Torr C_3H_6 + 25 Torr of H_2 +25 Torr of D_2 and 880 Torr of Ar) at 300 K.

poisoned the surface. Regardless, ethylene conversion and the HD spike are still observed.

In addition to saturating the surface of the Pt crystal with strongly adsorbed hydrocarbons, the reproducibility of the HD production trend was tested by substituting ethylene for propylene in the gas phase. The outcome of this experience is shown in Figure 5.5: propylene is hydrogenated twice as slow as ethylene and the HD inflection occurs at ~ 1700 s, roughly 300 s before propylene is fully hydrogenated.

The results from this section suggest that the behavior of the HD production trace is general and characteristic of the H-D scrambling that occurs during the catalytic hydrogenation of ethylene over Pt surfaces carried out at the experimental conditions used in this work.

5.2.3. Kinetics of ethylene hydrogenation vs. H-D scrambling.

Figure 5.6 compares the kinetics of ethylene hydrogenation using a 1:1 H_2/D_2 gas mixture with the HD production that occurs during the reaction. The product traces displayed in that figure were obtained after deconvoluting the raw data using a well-established method reported elsewhere [11] (Appendix 2). Following deconvolution, the ordinates axis was scaled and expressed in terms of TON (molecules* Pt $atom^{-1}$). The left frame of Fig. 5.6 shows the accumulation of HD as well as the consumption of both hydrogen and deuterium during the hydrogenation of ethylene. The consumption traces are in good agreement with the accumulation of HD, since they exhibit a steep decline that mirrors the inflexion point in the HD production trace. In addition, as deduced from Fig. 5.3, the HD turnover value at the end of the reaction is approximately double of the

final value for H_2 and D_2, which is expected for a reaction carried out with a gas mixture containing H_2/D_2 in a 1:1 ratio. The C_2X_6 trace in this panel was scaled by a factor of 10 to facilitate comparisons with the hydrogenation reaction.

The right panel of Fig. 5.6 shows the kinetic traces of ethane, its deuterated counterparts, and the total C_2X_6 trace, which is the sum of all the ethane traces. The linear accumulation of products and consumption of reactants are evidence of a pseudo zero order with respect to ethylene, as indicated before [12, 13, 14]. The total consumption of ethylene requires approximately 850 turnovers, similar to the amount reported in chapter 3 (900 turnovers) in the absence of deuterium.

By differentiating the traces from Fig. 5.6 and taking advantage of the fact that the reactor runs in batch mode, it was possible to calculate the rates of production and consumption of each species in terms of turnover frequencies (TOF = TON/s) and to express them as a function of time. The outcome of this procedure is displayed in Fig. 5.7. The left panel shows that the accumulation of HD is constant before its dramatic increase in rate at approximately 720 s, which is mirrored to a lesser extent by the consumption rates of hydrogen and deuterium. A closer inspection shows that the maximum in the HD rate is approximately twice the minimum of the absolute value of the H_2 and D_2 rates, a trend that is expected given the H_2/ D_2 gas mixture used. Additionally, in the early stages of the reaction there is a slight mismatch between the rates of H_2 and D_2 consumption and that of HD production. The rate of consumption seems to increase slightly with time while the rate of HD accumulation is fairly constant.

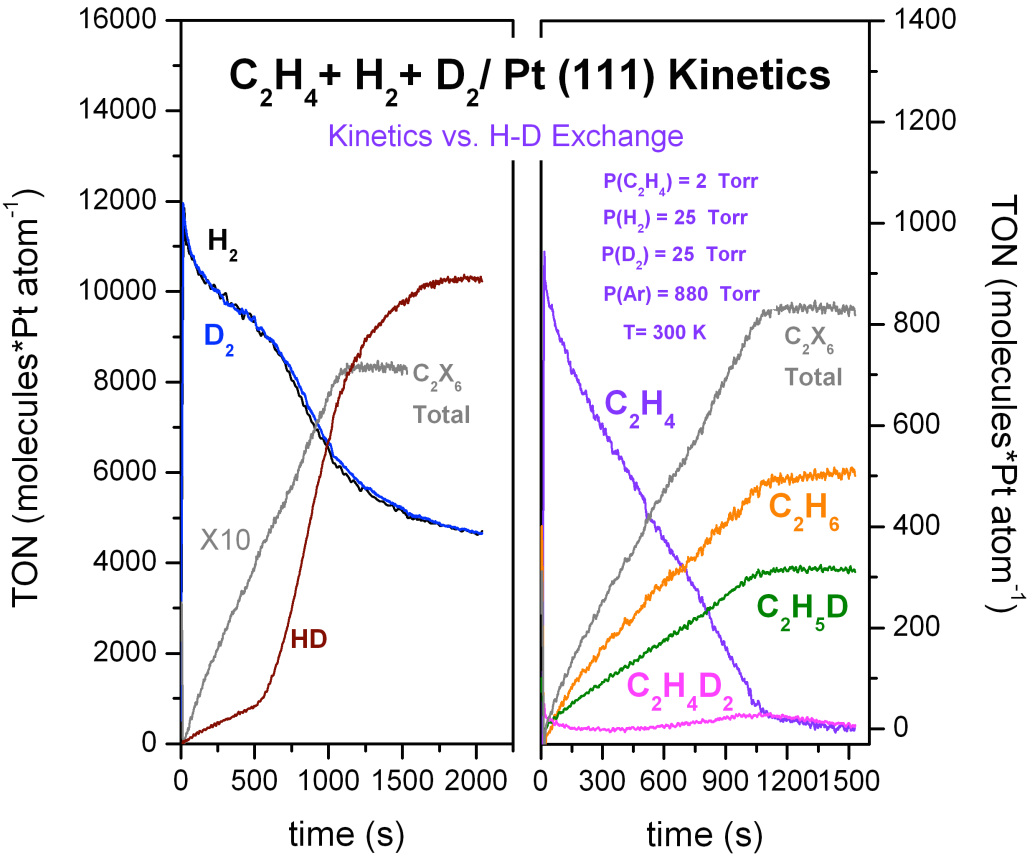

Figure 5.6. Comparison of the kinetics of ethylene hydrogenation vs. HD production, expressed in turnover numbers (TON), obtained after exposing a clean Pt (111) surface to a (2 Torr C_2H_4 + 25 Torr of H_2 + 25 Torr of D_2 and 880 Torr of Ar) at 300 K Left: HD production and hydrogen and deuterium consumption traces. Right: Kinetics of ethylene hydrogenation and H-D exchange.

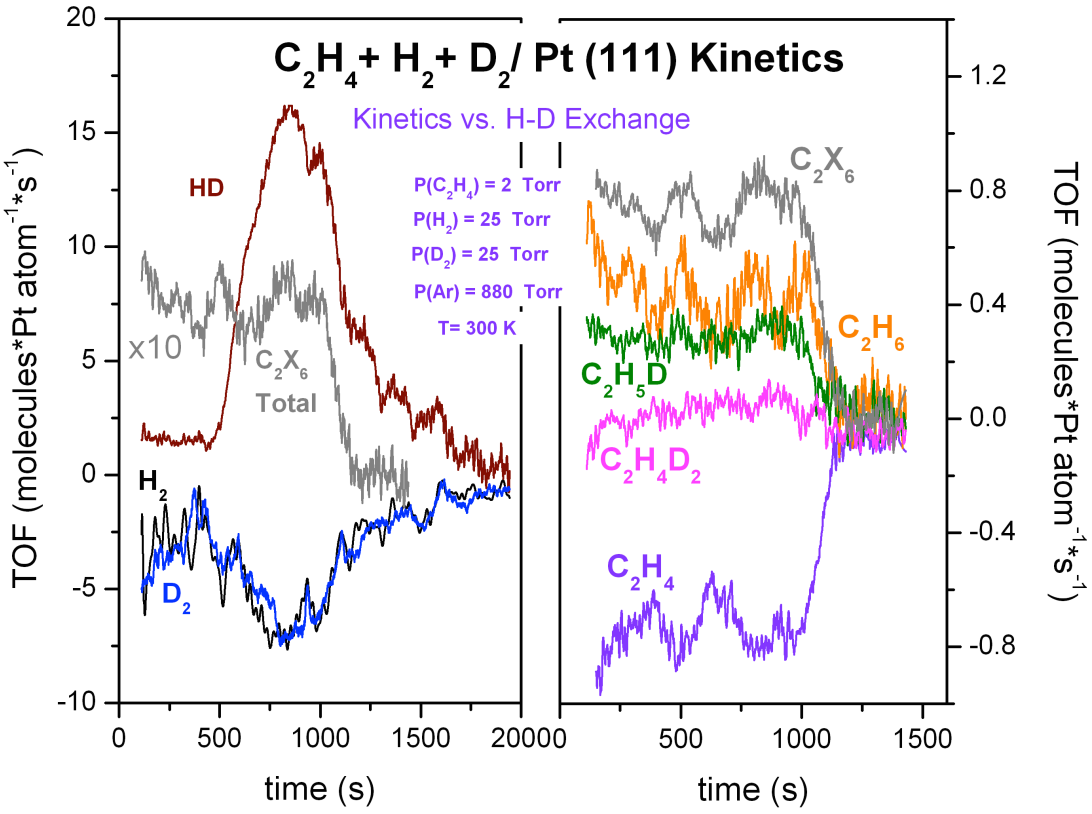

Figure 5.7. Ethylene hydrogenation kinetics vs. H-D exchange. Reaction rates expressed in turnover frequencies (TOF's) obtained by differentiating the product traces of Fig. 5.6. Left: HD production and hydrogen and deuterium consumption. Right: Kinetics of ethylene hydrogenation.

The right panel of Fig 5.7 displays the rates of production of C_2H_6, C_2H_5D, and $C_2H_4D_2$ and the total rate C_2X_6, which mirrors the consumption rate of ethylene within experimental error. All rates are fairly constant throughout the reaction until ethylene is completely depleted.

5.2.4. H-D scrambling kinetics vs. temperature.

The HD production transition was also studied as a function of reaction temperature. The relevant kinetic data are provided in Figure 5.8. As shown in the left frame of that figure, a small increase in temperature, from 300 K to 320 K, leads to the complete disappearance of the nonlinear transition: only the high-rate HD production regime is seen at the latter temperature or above. The rates for each temperature were calculated from the TON on the left panel and were expressed as TOF over time in the right frame of Fig. 5.8. The time scale in that panel is expanded in the 0 to 300 s time range since it is there where most of the data for the product traces on the left frame are seen. The decrease in rates seen in the early stages of the runs at 340, 350, and 360 K is due to the rapid accumulation of HD, which saturates after approximately 100 s and is followed by a slow down because of the low pressures of reactants remaining in the gas phase. The bottom frame of Fig 5.8 displays an Arrhenius plot of the Ln (TOF/ HD molecules* Pt atom* s^{-1}) vs. (1/T)/ K^{-1}. The information gathered from this analysis shows that the H-D scrambling is an activated process on the surface of the working catalysts with an energy barrier of 12.7 ± 0.7 kcal/mol. This barrier is comparable to the 15.6 ± 0.5 kcal/mol found for H-D scrambling over a clean Pt (111) surface with molecular beams experiments [23]. Unfortunately, since no transition is seen in these

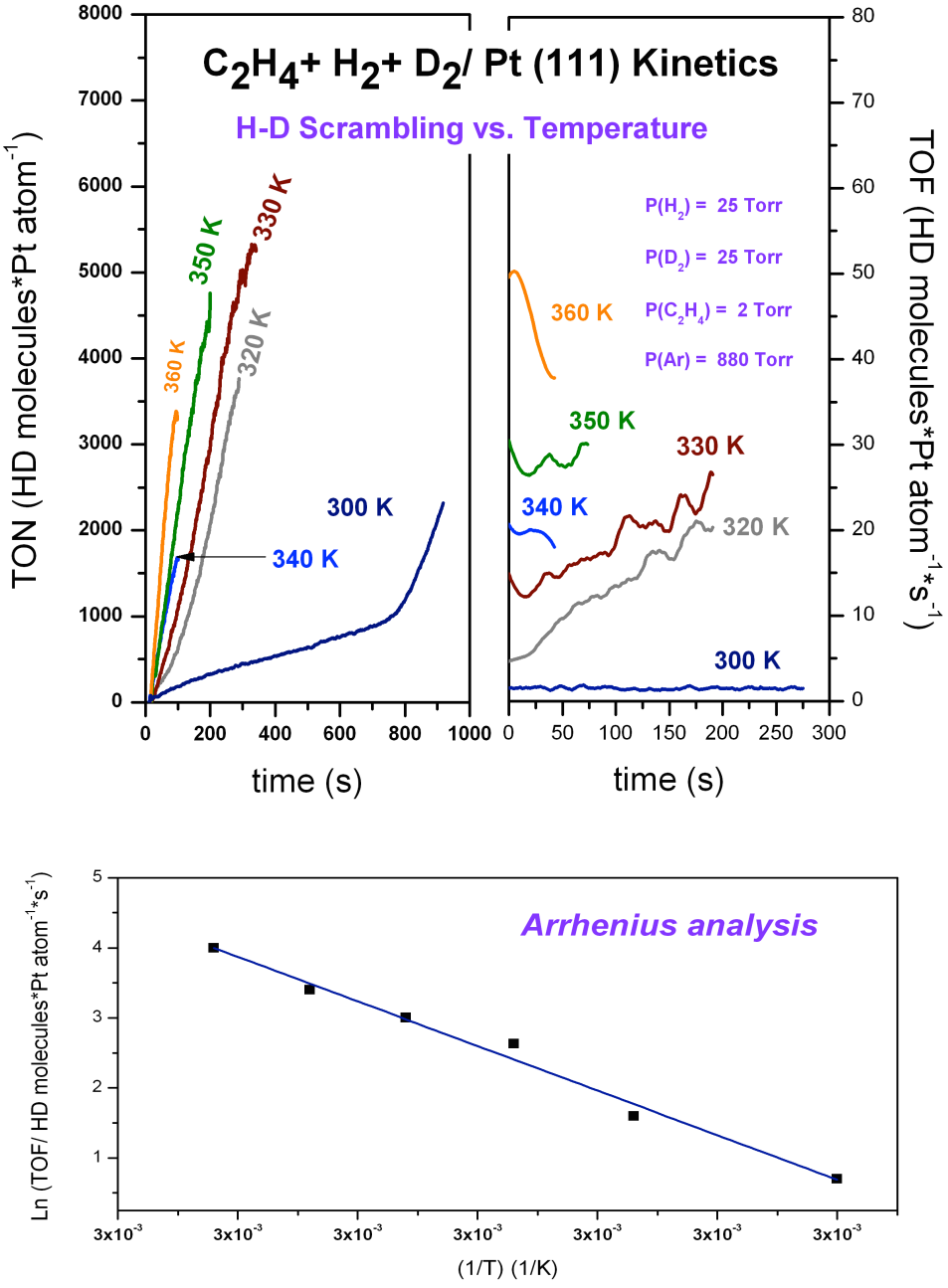

Figure 5.8. HD production vs. Temperature. Top left: HD accumulation, expressed in turnover numbers (TON), as a function of temperature. Top right: reaction rates, expressed in turnover frequencies (TOF's), as a function of temperature. Bottom: Arrhenius plot in terms of the Ln (TOF/ HD molecules *Pt atom^{-1} * s^{-1}) vs. (1/T) K.

curves (other than at 300 K), they do not provide information regarding the H-D spike. It would appear that such transition happens at too early a reaction time to be captured by our measurements.

5.2.5. CO titration of bare Pt sites during the catalytic hydrogenation of ethylene with a 1:1 H_2/D_2 gas mixture.

The sudden increase in the HD production rate vs. time shown in Fig. 5.7 bares resemblance to the explosive increase in reaction rates exhibited by autocatalytic systems [15-19]. These so-called surface explosion kinetics are characterized by the rapid decomposition of adsorbates leading to an exponential growth in vacant reactive sites. So, by following the evolution of bare Pt sites during the catalytic hydrogenation of ethylene it should be possible to determine if the behavior displayed by the HD accumulation trace is due to this type of phenomena. To achieve this, the reaction was quenched with a CO (30 Torr)/ Ar (700 Torr) gas mixture at different times, focusing on the vicinity of the HD production trace inflection point. The assumption is that one CO molecule is chemisorbed per bare Pt atom [20], poisoning any further progress of the catalytic hydrogenation and HD production reactions. The reliability of the RAIRS C-O stretch peak at 2079 cm^{-1} for atop CO adsorption on Pt surface atoms and the bridge-bonded peak at 1890 cm^{-1} on metal surfaces under UHV conditions make CO a great titrating agent for bare Pt sites [21]. Since the intensity of the IR peaks is typically directly proportional to the amount of the adsorbate, the intensity of the CO peak at 2079 cm^{-1} should be representative of the surface concentration of bare Pt sites during the hydrogenation reaction of ethylene over

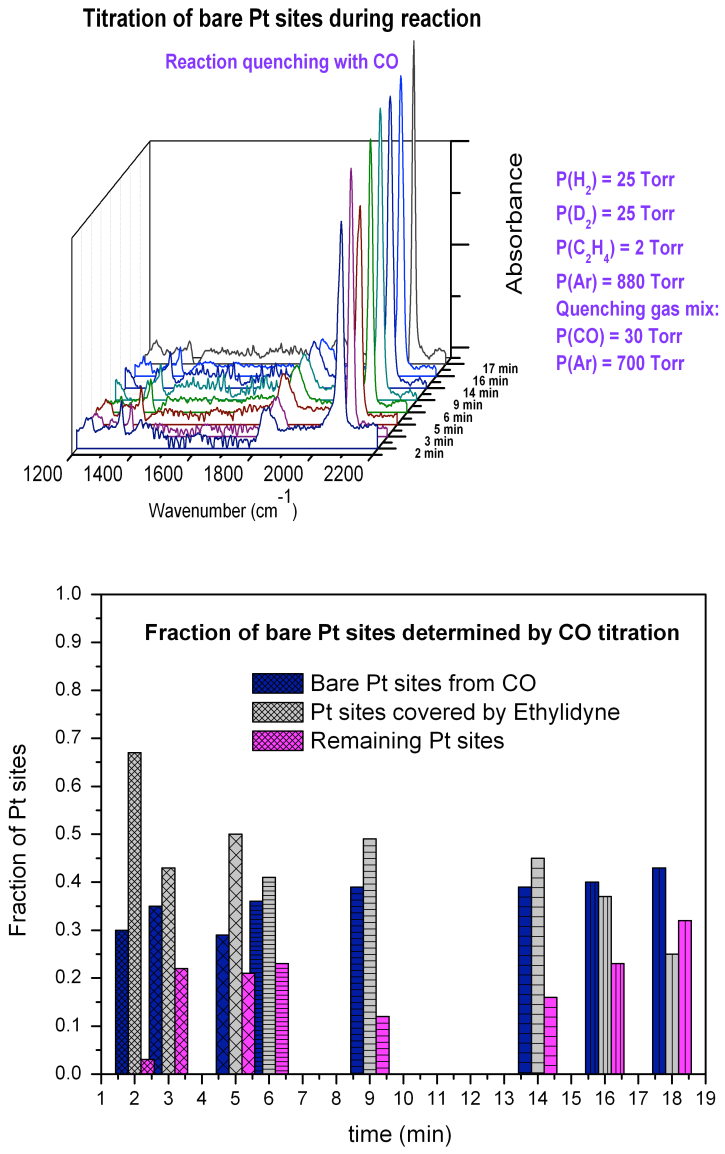

Figure 5.9. Titration of bare Pt sites with CO before, during and after the HD spike. Top: RAIRS spectra collected after quenching the catalytic hydrogenation of ethylene with a gas mixture of (30 Torr of CO + 700 Torr of Ar). Bottom: column plot of the fraction of Pt sites covered by CO, ethylidyne and those that are not covered by either species.

Pt (111) at the time of the quenching (for the case of adsorbed CO there is a known deviation from linearity between coverage and RAIRS intensity in the high-coverage end [21], but that is not too significant for the studies reported here). The upper frame of Figure 5.9 shows the RAIRS spectra collected after the reaction was quenched at several times. These IR results were used to estimate the fraction of Pt sites that were covered by CO and ethylidyne at different times during the reaction. The fraction of bare Pt sites determined by CO only varies by 0.1 from beginning until reaction completion, as can be clearly appreciated in the bottom frame of Fig. 5.9. This only represents 10% of the coverage obtained when CO is adsorbed under UHV conditions in our system. Such a low increment in bare Pt sites cannot explain the explosive growth in reaction rates observed for the H-D exchange. Moreover, Fig. 5.9 also shows the remaining Pt sites that are unaccounted by CO or ethylidyne during the reaction. These sites represent approximately 23 % of the surface that could presumably be available for H-D scrambling; yet this reaction is still limited for the first 720 s. These observations ruled out a surface explosion as the source of the HD spike.

5.2.6. Specific surface site blocking with propane-1-thiol.

Previous studies have shown that the hydrogenation of ethylene is site specific, occurring almost in its entirety on the terrace sites of the Pt surface [22]. Contrarily, molecular beam studies with H_2/ D_2 gas mixtures displayed increased production of HD when the beam is aimed at surface defect sites [23], which suggests that the dissociative adsorption of hydrogen is also site specific [24]. Considering these observations, it was hypothesized that the spike in HD accumulation curves seen here might have been related

to a sudden accessibility of defect sites during the catalytic hydrogenation of ethylene over Pt (111). According to this, if the defect sites on the surface were selectively blocked, then the inflection in the HD production trace would not occur. Since previous reports have found that sulfur and sulfur-containing hydrocarbons bind preferentially to defect sites on the Pt surface [25, 26], propane-1-thiol was used as a sulfur source to block the defect sites of the single crystal in the experiments carried out in this section. The experimental procedure entailed dosing a small amount of the thiol under UHV conditions followed by annealing of the prepared surface to 725 K to decompose the adsorbate, leaving only the sulfur on the defect sites. The expectation is that this selective site blocking should stop any possibility for defects sites to become available for increased HD production at any time during the hydrogenation reactions. Figure 5.10 shows the results obtained from these experiences. The left panel is shown simply as reference and it is taken from Fig. 5.2. The middle panel of the figure exhibits the results for a thiol exposure of 0.1L, and illustrates how an exposure of this magnitude is unsuccessful at blocking the defect sites since the HD accumulation trace remains unaltered. The right panel of Fig. 5.10 shows the other extreme of this poisoning, to an extent that affects the ethylene hydrogenation reaction as well. The extent of the poisoning is considerable in this case, since even after 3000 s the reaction has not reached completion. These results are not sufficient to fully discard the initial hypothesis of different sites for ethylene hydrogenation and HD production reactions, but are quite suggestive that this may not be the explanation for the non-linear behavior, since no evidence is seen in these data for selective poisoning of one reaction over the other.

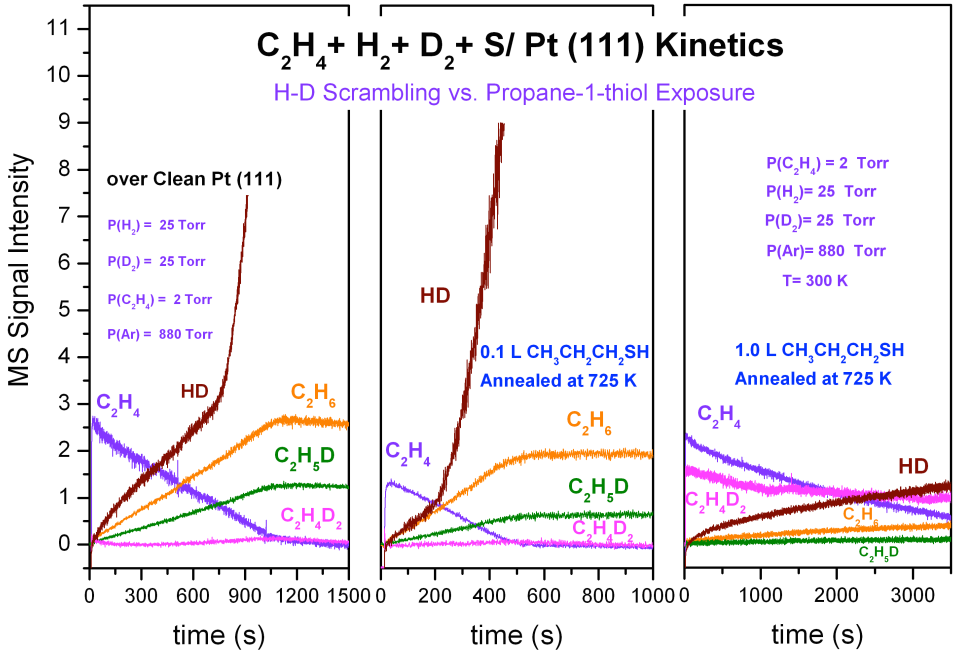

Figure 5.10. HD production and ethylene hydrogenation vs. propane-1-thiol exposure. Kinetics obtained after exposing surfaces to a (2 Torr C_2H_4 + 25 Torr of H_2 +25 Torr of D_2 and 880 Torr of Ar) at 300 K. Left: Reference of H-D scrambling over a clean surface (left panel from Fig. 5.2). Middle: Conversion over a Pt (111) surface exposed to 0.1 L of propane-1-thiol annealed at 725 K. Right: Conversion over a Pt (111) surface exposed to 1.0 L of propane-1-thiol annealed at 725 K.

5.2.7. H-D Exchange vs. ethylene pressure.

According to the results in section 5.2.1, in the absence of ethylene the HD production does not show a non-linear behavior. This confirms the initial slow-rate regime for HD production as associated with the presence of the olefin in the gas phase.

Our next approach was to study in more detail how the HD production trace inflection point is affected by changes in the pressure of ethylene in the gas mixture while maintaining the hydrogen and deuterium pressures unaltered. The results of these experiences are shown in Figure 5.11 where, aside from 2 Torr (the data discussed before), 1, 3 and 5 Torr of ethylene were used. The first observation that derives from these new traces is that greater amounts of ethylene increase the reaction completion time for ethylene hydrogenation and the time at which the H-D spike occurs even though H_2 and D_2 are in considerable excess. Conversely, the use of ethylene pressures less than 2 Torr decrease the time at which the inflection occurs, making it almost undetectable. A close inspection of Fig. 5.11 yields Fig. 5.12. The left frame of this figure reveals that the inflection in HD *always* occurs when less than 1 Torr of ethylene remains in the gas phase. However, this panel does not show a clear trend that can relate the ethylene pressures at the inflection with the initial ethylene pressure. The right panel of Fig. 5.12 exhibits a better trend that relates the initial pressure of ethylene with the percent of olefin conversion at the moment of the spike. It is evident that with increasing ethylene pressures more of it needs to be consumed in order for the H-D accumulation increase to occur. This result might explain why this non-linearity in H-D scrambling kinetics has

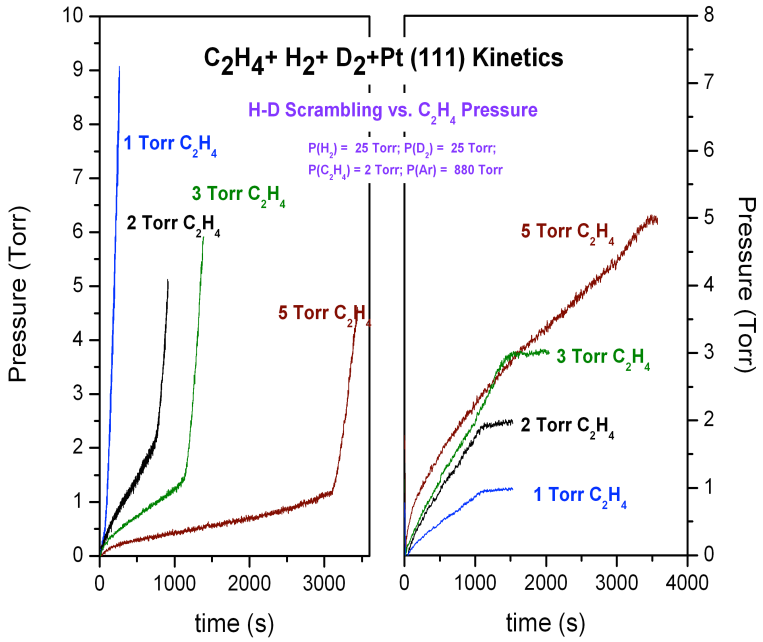

Figure 5.11. HD production vs. initial ethylene pressure. Kinetics obtained after exposing a clean Pt (111) surface to a (X Torr C_2H_4 + 25 Torr of H_2 +25 Torr of D_2 and 880 Torr of Ar) where X= (1, 2, 3, 5) at 300 K. Left: H-D accumulation traces. Right: Ethane accumulation traces.

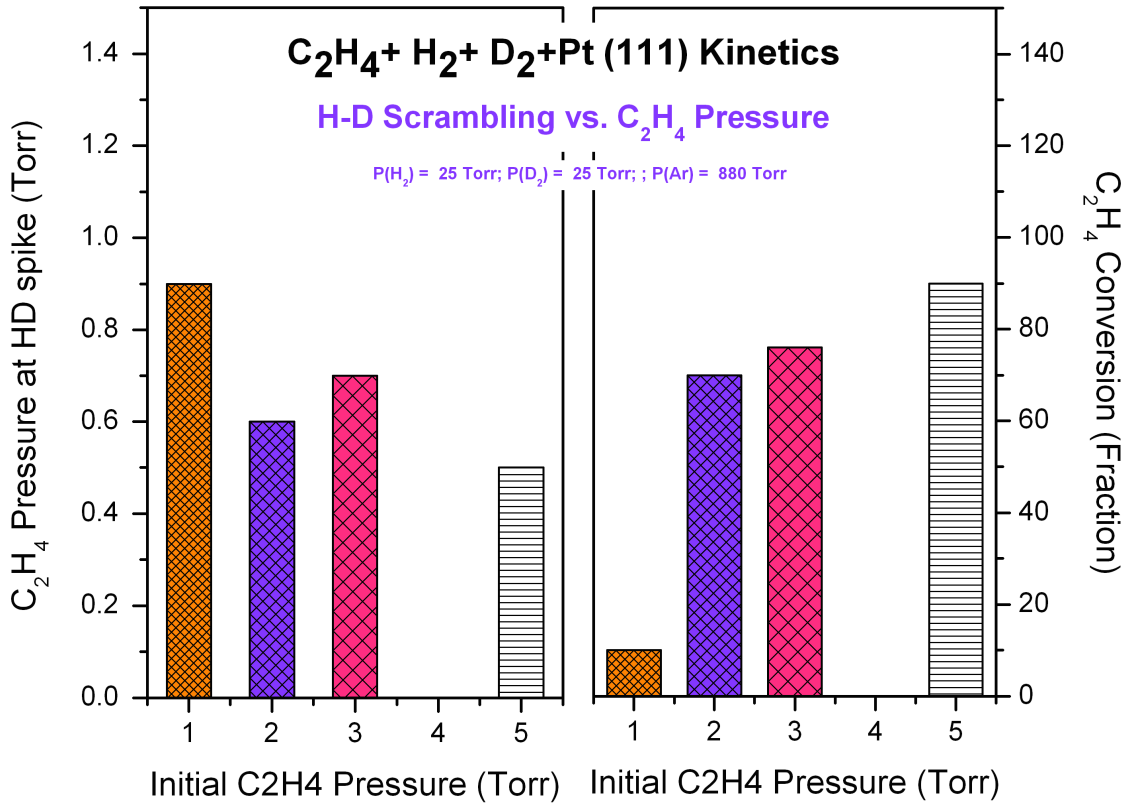

Figure 5.12. Right: Column plot relating the ethylene pressure at the HD production spike point with the initial ethylene pressure. Left: Column plot relating the fraction of converted ethylene at the H-D spike with the initial olefin pressure. Pressures were obtained from the kinetics recorded after exposing a clean Pt (111) surface to a (X Torr C_2H_4 + 25 Torr of H_2 +25 Torr of D_2 and 880 Torr of Ar) where X= (1, 2, 3, 5) at 300 K.

not been observed previously, since most studies [7, 8, 9] that performed experiments with $H_2 + D_2$ mixtures employed ethylene pressures of approximately 30 Torr.

The results from this section define a clear threshold for the H-D spike and suggest that at ethylene pressures below 1 Torr the dissociation of hydrogen on the metal surface is no longer the rate-limiting step of the hydrogenation reaction.

5.2.8. In-situ re-start reactions.

The results documented in section 5.2.7 suggest that the transition in HD production reaction being discussed in this chapter hinges on the value of the ethylene pressure in the gas phase. The threshold seems to occur at ethylene pressures of approximately 1 Torr; below that value, the HD production only shows the fast-rate regime regardless of the initial ethylene pressure (Fig 5.11).

Our next test was designed to check if this transition between the two HD production regimes is reversible. These re-start experiments were performed by topping off the existing reaction mixture with a fresh amount of ethylene after the occurrence of the HD spike during the initial run for the hydrogenation of ethylene with a gas mixture as the one described in chapter 3. The olefin was added as a 930 Torr C_2H_4/Ar gas mixture, which yielded a 720 Torr working pressure upon expansion in the loop. The outcome of these experiences is depicted in Figure 5.13. The frame on the left shows the consequence of adding an extra ethylene pressure of 2 Torr mixed with 928 Torr of Ar after 940 s of reaction, soon after the HD production rate transition, which in this case is seen at 700 s. Only a slight indent is observed in the HD production trace at around 1000 s, which is readily mitigated in the following ~100 s. This indicates that the posterior

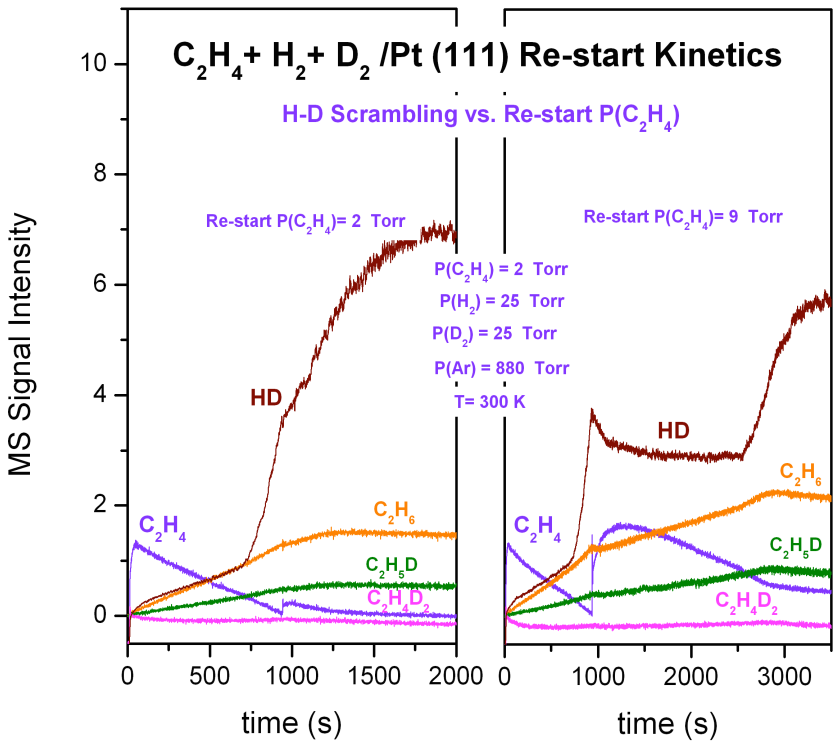

Figure 5.13. Effect of topping off the reaction mixture with additional ethylene on HD production. Kinetics obtained after exposing a clean Pt (111) surface to a (2 Torr C_2H_4 + 25 Torr of H_2 +25 Torr of D_2 and 880 Torr of Ar) at 300 K. Left: Top off with $P(C_2H_4)$ = 2 Torr after 940 s of reaction. Right: Top off with $P(C_2H_4)$ = 9 Torr after 935 s of reaction.

addition of small amounts of the olefin to the reaction mixture do not have a long lasting effect on the HD trace after its inflection. On the other hand, the trace for ethylene indicates that the partial pressure for that reactant was augmented in this case from 0.06 Torr to 0.30 Torr, well below the 1 Torr threshold where the HD production trace inflexion point is seen. It is quite likely that the added ethylene in this case was not sufficient to revert to the early HD production regime. It is also worth noting that a close inspection of the product trace shows a slight decrease in the HD accumulation slope. Nonetheless, this might be associated to the dilution caused by the addition of extra argon. The same decrease in the slope is displayed in the ethane traces and its deuterated counterparts, although to a lesser degree.

The right panel of Fig. 5.13 exhibits the effects of introducing an ethylene/argon mixture comprised of 9 Torr of the olefin and 921 Torr of the ballast gas after 935 s of reaction (the HD production rate transition occurring at 715 s). With this topping off ethylene pressure there is a clear effect on the HD production reaction: the addition of a greater amount of the olefin basically hinders the HD accumulation, as seen in the interval between 1000 and 2500 s. The production of ethane, C_2H_5D and $C_2H_4D_2$ also slow down considerably, but this could be the result of the dilution of the gas phase due to the extra ballast gas added. For this particular case it might be possible that the sum of the freshly introduced ethylene and the unreacted ethylene surpassed the $P(C_2H_4)$ used at the beginning of the experiment, establishing a pressure regime comparable to the one reported for 5 Torr of ethylene in Fig. 5.11. The second transition in HD accumulation is observed at 2552 s, when the partial pressure of ethylene is ~ 0.47 Torr, which is similar

to the partial pressure of olefin at the first inflection: ~ 0.45 Torr. This observation shows that switch in kinetics evidenced by the H-D scrambling is reversible and hinges on the pressure of ethylene in the gas phase during reaction.

5.3. Discussion.

The high-pressure catalytic hydrogenation of ethylene carried out with a 1:1 H_2/ D_2 mixture over a Pt single crystal displayed a pseudo zero order on ethylene which is evidenced by the linear kinetics shown in Fig. 5.2 and by the approximately constant turnover frequencies presented in Fig 5.7, all in good accordance with the findings of previous studies [5]. Surprisingly, this reaction, performed under high H_2 (D_2): C_2H_4 ratios, revealed an unprecedented behavior for the HD accumulation, characterized by a dramatic increase in its reaction rate that occurs well before the catalytic hydrogenation has reached completion. This inflection in the HD accumulation trace will be referred to as the "HD spike" throughout this section. Given the explosive behavior of this phenomenon, it was initially hypothesized that its occurrence was due to an exponential growth of bare Pt sites during the catalytic hydrogenation of ethylene, which is characteristic of autocatalytic systems. Nevertheless, the results obtained from CO surface site titrations at different times (Fig 5.9) rebuked this hypothesis, since the total change in Pt sites represents only 10% of the total bare sites, an amount that does not correlate with the exponential increase of the rate of HD production.

Alternatively, it was considered that the HD spike was associated with the presence of defect surface sites, given that previous reports of molecular beam

experiments [23] showed that the HD exchange occurs specifically on these sites. However, although the attempts to explore this hypothesis were not conclusive, since the sulfur source (propane-1-thiol) used to preferentially block these sites was not well suited for the task (low exposures –0.1 L– did not hinder the HD production as expected, and higher exposures –1 L– poisoned all reactions), the data we acquired suggests that this may not be a good explanation either.

The most interesting results from this study of the HD production are those presented in sections 5.2.7 and 5.2.8. In conjunction, the results from these sections provide compelling evidence that the accumulation of HD during the catalytic hydrogenation of ethylene over Pt (111) is strongly dependent on the total pressure of ethylene before, during, and after the HD spike. This can be appreciated in Figs. 5.11, 5.12, and 5.13. Also, it is worth noting that even if the results from Fig. 5.11 do not show a clear trend that relates the ethylene pressure at the HD spike and the starting pressure of C_2H_4 (perhaps because of the large experimental errors associated with these measurements), it undoubtedly establishes a threshold at which the HD spike occurs: at ethylene pressures below 1 Torr. These findings represent crucial pieces of information that are characteristic of the behavior of the HD production reaction.

The IR spectra from section 5.2.5 provide a very detailed insight on the behavior of the ethylidyne layer on the surface during reaction. From Fig. 5.9 its is clear that, as time passes during the catalytic conversion of ethylene to ethane, the ethylidyne layer that readily adsorbs is slowly consumed, a fact that is evidenced by the decrease in the signal intensity of the methyl deformation mode at 1340 cm^{-1}, and by the parallel increase of the

C-O stretching mode of carbon monoxide at 2079 cm^{-1}. This confirms that towards the end of the reaction the surface is seemingly devoid of ethylidyne.

The results from section 5.2.1 and 5.2.2 suggest that the sudden increase in the rates of HD production occurs regardless of the nature of the adlayer covering the surface (except for complete surface poisoning), and it is reproducible in the hydrogenation of other olefins. It is worth mentioning that the composition of the final gas mixture shows the expected statistical distribution of amu 2, 3 and 4 expected from the stoichiometry of the reaction $H_2 + D_2 \rightarrow 2\ HD$ when a 1:1 H_2/ D_2 is used.

The non-linearity of the HD accumulation shown in this chapter reveals the existence of two major kinetic regimes during the catalytic hydrogenation of ethylene. The threshold to transfer from one kinetic scheme to the other is defined by the pressure of ethylene in the gas phase (~1 Torr). In the first kinetic regime (P (C_2H_4)> 1 Torr), the HD production is limited by the presence of the olefin. This is consistent with previous reports [7, 8, 9] where H_2/ D_2 mixtures were used in the hydrogenation of ethylene. Our findings are also in accordance with results obtained by tracking the *ortho-para* hydrogen conversion in the presence and absence of this hydrocarbon [7]. This study showed that the *para* hydrogen conversion needed 13 minutes to reach completion in the absence of ethylene and 119 minutes in its presence. The interpretation of these observations is that at pressures of ethylene above 1 Torr the dissociation of hydrogen on the metal surface is the rate-limiting step of the hydrogenation reaction. The second kinetic regime (P (C_2H_4)< 1 Torr) is characterized by fast HD production and seemingly unaltered ethylene conversion. Since no delay is observed in the H-D scrambling we presume that the

hydrogenation of ethylene is no longer limited by the dissociation of hydrogen on the surface. This fact might be able to fill the reactivity gap between reactions carried out at atmospheric pressures and UHV conditions.

Using the information gathered in this chapter we explain the sharp transition between reaction schemes as follows: early in the reaction (when $P(C_2H_4)$> 1 Torr) the surface of the metal is covered by ethylidyne, hydrogen and physisorbed ethylene. Hydrogen and ethylene share the bare Pt sites estimated with CO titration from Fig.5.9. As the reaction progresses HD and ethane are being produced simultaneously, however the presence of the olefin and the alkylidyne on the surface hinder the diffusion of H and D atoms delaying the formation of HD. While ethylene is being consumed the fraction of bare Pt sites varies very little (Fig. 5.9), but the distribution of these sites is changing, meaning that the bare Pt islands are slowly increasing in size. When the pressure of ethylene in the gas phase decreases below 1 Torr its coverage on the surface also decreases and these bare Pt islands are of a size that allows the free diffusion of H and D atoms provoking the sharp spike in HD production regardless of the remaining ethylene and ethylidyne.

5.4. Conclusions.

At high H_2 (D_2): C_2H_4 ratios (= 25), the HD production reaction displays non-linear kinetics during the atmospheric-pressure hydrogenation of ethylene over Pt (111) crystals. It was determined that this so called HD spike always occurs when the pressure of ethylene in the gas phase is less than 1 Torr. In addition, the HD production reaction

shows a strong dependence with the pressure of ethylene, since the accumulation of HD occurs at a slower rate at higher starting C_2H_4 pressures. More significantly, the sudden increase in reaction rate displayed by the HD accumulation can be reverted by the addition of a fresh batch of ethylene ($P(C_2H_4) \sim 9$ Torr). All these findings suggest that the HD kinetic spike is mostly controlled by the pressure of the olefin in the gas phase rather than by changes in ethylidyne coverage that are occurring on the surface throughout the reaction.

Even though most of the results in this chapter point to the fact that the gas-phase ethylene exerts most of the control over the HD spike, effects from the surface cannot be completely discarded, since the attempts to block surface defects sites were not completely successful. In order to establish unequivocally that the changes in ethylene pressure are solely responsible for the behavior of the HD accumulation, it is necessary to show that surface defect sites do not play a crucial role in this behavior. The poisoning experiences should be repeated with a more reliable sulfur source such as SO_2 or H_2S.

The findings from sections 5.2.1 and 5.2.2 suggest that the non-linear kinetics of the HD production reaction are general and can be found for other reactions under the right experimental conditions, since (at least for small linear olefins) is does not discriminate against the nature of the gas-phase olefin or the nature of strongly adsorbed hydrocarbon adlayer.

Finally, and of more consequence, the nonlinearity of the HD accumulation trace is evidence of the existence of two mechanistic schemes for the hydrogenation of ethylene on Pt (111): the first one occurs at $P(C_2H_4) > 1$ Torr and is limited by the

dissociative adsorption of hydrogen on the metal surface and the second one occurs at $P(C_2H_4)< 1$ Torr and is not limited by this step. The first reaction scheme is in good agreement with previous findings of studies done with H_2 and D_2 mixtures and with *ortho-para* hydrogen conversion experiments, and the second kinetic regime is reported for the first time in this work.

5.5. References.

[1] Zaera F., *Phys. Chem. Chem. Phys* **2013**, 15, 11988-12003.

[2] T. V. W. Janssens and F. Zaera, *J. Phys. Chem*., **1996**, 100, 14118.

[3] Ohtani T.; Kubota, J.; Kondo, J.N.; Hirose, C. and Domen, J., *J. Phys. Chem. B*, **1999**, 103, 4562.

[4] Salmerón, M. and Somorjai, G.A., *J. Phys. Chem*., **1982**, 86, 341.

[5] Tillekaratne, A., Zaera, F., *Surf. Sci.* submitted for publication.

[6] Zaera, F. and Somorjai, G.A., *J. Am. Chem. Soc*, **1984**, 106, 2288-2293.

[7] Twigg, G.H, *Dissc. Faraday Soc.*, **1950**, *8*, 152.

[8] Bond G.C.; Phillipson J.J.; Wells P.B.; Winterbottom, J.M., *Trans. Faraday Soc.*, **1964**, 60, 1847-1864.

[9] Farkas, A.; Farkas, L. *J. Am. Chem. Soc.* **1938**, *60*, 22.

[10] Rekoske, J.E.; Cortright, R.D; Goddard, S.A.; Sharma., B.S.; Dumesic, J.A., *J. Phys. Chem.*, **1992**, *96* (4), 1880–1888

[11] Wilson J.; Guo, H.; Morales, R.; Podgornov, E.; Lee, I.; F. Zaera, *Phys. Chem. Chem. Phys.*, **2007**, *9*, 3830-3852.

[12] Horiuti, J.; Miyahara, K. "*Hydrogenation of Ethylene on Metallic Catalysts*," National Bureau of Standards, **1968**.

[13] Bond, G. C. *Metal-Catalysed Reactions of Hydrocarbons*; Springer: New York, **2005**.

[14] Cortright, R. D.; Goddard, S. A.; Rekoske, J. E.; Dumesic, J. A., *J. Catal.* **1991**, *127*, 342-353.

[15] McCarty, J., J. Falconer, and R.J. Madix, *J. Catal.*, **1973**, *30*, 235- 249.182

[16] Falconer, J. and R. Madix, *Surface science*, **1974**, *46*, 473-504.

[18] Lesley, M. and L. Schmidt, *Chem. Phys. Lett.*, **1983**, *102*, 459-463.

[17] Paul, A., C.J. Jenks, and B.E. Bent, *Surf. Sci.*, **1992**, *261*, 233-242.

[19] Behzadi, B., et al., *J. Am. Chem. Soc.*, **2004**. 126, 9176-9177.

[20] Surface Area and Porosity," Chap. 6. Academic Press, New York, 1967; Sinfelt, J. H., and Yates, D. J. C., *J. Catal*., **1968** *10*,362; Vannice, M. A., *J. Catal*., **1975**, *37*,449; Innes, W. B., in "*Experimental Methods in Catalytic Research*" (R. B. Anderson, Ed.), Vol. 1. Academic Press, New York,**1968**; Moss, R. L., in "*Experimental Methods in Catalytic Research*" (R. B. Anderson, Ed.), Vol. 2. Academic Press, New York, **1972**.

[21] Hughes, T. R., Houston, R. J., and Sieg, S. P., Ind. Eng. Chem. Process Des. Dev. 1, 96 (1962).

[22] Somorjai, G.A. and Li, Y., *Introduction to Surface Chemistry and Catalysis, Second Edition*, Wiley, **2010**, p. 586.

[23] Salmeron, M.; Gale, R. J.; Somorjai, G. A., *J. Chem. Phys.* **1977**, *67*, 5324-5334.

[24] Groot, I. M. N.; Kleyn, A. W.; Juurlink, L. B. F., *J. Phys. Chem. C* **2013**, *117*, 9266 9274.

[25] Streber, R.; Papp, C.; Lorenz, M.P.A.; Höfert, O.; Darlatt, E.; Bayer, A.; Denecke, R.; Steinrück, H.-P., *Chem. Phys. Lett.*, **2010**, *494*, 188-192.

[26] Koestner, R.J.; Salmeron, M.; Kollin, E.B.; Gland, J.L., *Surf. Sci.* **1986**, *172*, 668.

CHAPTER 6: KINETIC STUDY OF THE CATALYTIC HYDROGENATION OF ETHYLENE OVER Pt (111) CRYSTALS IN THE mTorr OLEFIN PRESSURE REGIME.

6.1. Introduction.

This chapter presents some insight regarding the chemistry involved in the catalytic hydrogenation of ethylene on Pt single crystals in the mTorr ethylene pressure regime. It has been reported in the literature that even though this reaction displays turnover frequencies of approximately 1-10 ML/s under typical reaction conditions, they are slow in terms of reaction probabilities, where only 1 in $1x10^6$ collisions is reactive if 1 Torr of the reacting gas is used [1]. Also, since the reaction exhibits negative kinetic orders with respect to the olefin, it has been hypothesized and proven that under low olefin pressures the hydrogenation of ethylene displays reaction probabilities near unity [2]. The results shown in this chapter were used to complement the molecular beam findings of this study.

6.2. Results.

6.2.1. Catalytic hydrogenation of ethylene with olefin pressures in the mTorr and sub mTorr range.

The RAIRS spectra and product traces collected by using diluted mixtures of the olefin are shown in Figure 6.1. The spectra displayed the same fundamental ethylidyne features that are exhibited when the experiment is carried out at atmospheric or near

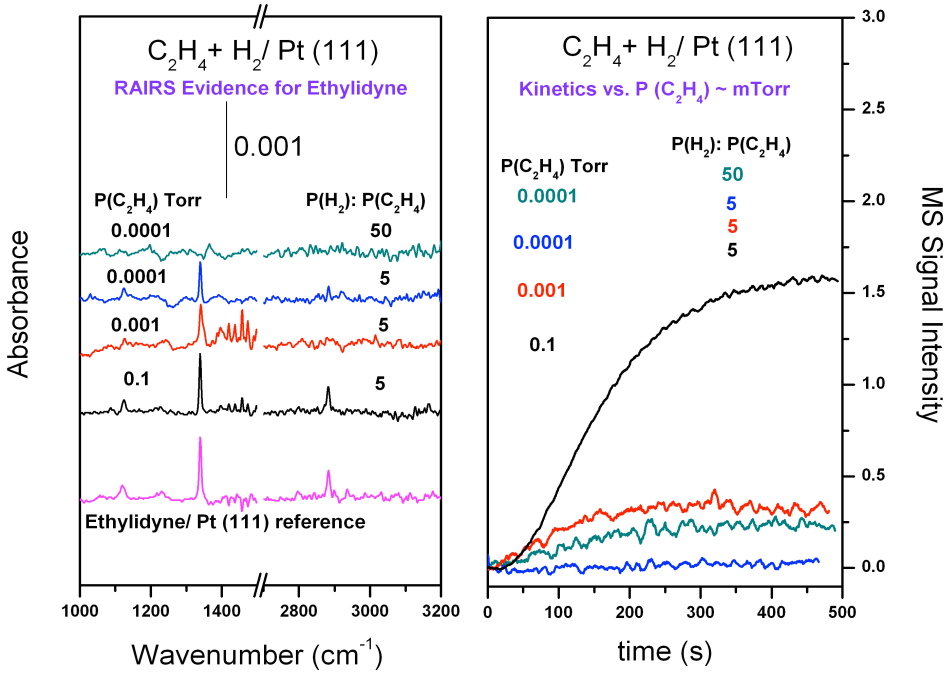

Figure 6.1. Left: RAIRS spectra obtained 10 minutes after evacuation of the HPC upon reaction completion. The spectra correspond to ethylene in different pressure ranges but same hydrogen to olefin ratios (except for the top spectrum). Right: Corresponding product traces of 30 amu for the RAIRS spectra shown in the left panel.

atmospheric pressures [1, 3, 4] mainly: the methyl symmetric deformation at 1340 cm^{-1}, the C-H symmetric stretching at 2881 cm^{-1} and the C-C stretching at 1123 cm^{-1} [5, 6, 7], as depicted in Figure 6.1. The intensity of the 1340 cm^{-1} band from the spectrum obtained with a 0.1 Torr of ethylene reveals a coverage near saturation. As the dilution factor increases ethylidyne is present at 66 % of its saturation coverage for those mixtures where the H_2:C_2H_4 = 5 (~20% more than what is measured in a typical hydrogenation experiment in this work). However, when the relative H_2 pressure is increased by one order of magnitude, the alkylidyne coverage decreases dramatically, and in some cases (like in Figure 6.1), it cannot be appreciated, showing that with greatly diluted gas mixtures increasing the H_2: C_2H_4 ratio not only promotes a faster hydrogenation of ethylene, but also helps in the removal of strongly adsorbed hydrocarbons, exposing more Pt sites for the catalytic conversion.

The right panel of Fig. 6.1 shows the product traces that correspond to each spectrum in the left panel. With an ethylene pressure of 0.1 Torr and a H_2: C_2H_4 = 5 it is still possible to track the formation ethane, which displays a steady increase until reaction completion. Nonetheless, an increase in the dilution factor seems slow down the hydrogenation reaction up to a point that it can no longer be appreciated when the mixture has been diluted ten thousand times. It seems that a way to revert this effect is by increasing the H_2: C_2H_4 to 50, which not only boosts the conversion of ethylene but also avoids the deposition of ethylidyne or promotes its removal.

6.3. Discussion.

Despite the instrumental limitations in performing experiments with diluted gas mixtures addressed in chapter 2, Figure 6.1 represents the most useful and reproducible information gained from the experiments carried out in this section. The RAIRS spectra shown were used to complement a molecular beam study [2] that employed H_2:C_2H_4 similar to the ones used with the operando setup of this work. In that study, greater ethylidyne coverage was associated with lower reaction probabilities in experiments where H_2:C_2H_4 = 5. However, when H_2:C_2H_4 was increased to 50, the reaction probabilities also increased. This trend was associated with the decrease in ethylidyne coverage due to the higher pressure of H_2. Similar results are obtained for the product traces displayed in this chapter although we also report a decrease in the conversion of ethylene which is not only associated to the presence of ethylidyne but also to the fact that the mixture is greatly diluted with Ar. An interesting fact that stems from the observations of this section is that, by increasing the hydrogen:ethylene ratio by a factor of ten under diluted conditions, the hydrogenation reaction seems to take place over a seemingly clean surface, a trend that is not observed at atmospheric or near atmospheric reaction pressures.

In chapter 5 we reported that the hydrogenation of ethylene at pressures below 1 Torr is no longer limited by the dissociative adsorption of hydrogen on the metal surface. This means that in the pressure regime studied here the hydrogenation of ethylene might be limited by another step that can easily lead to the formation of ethylidyne if greater pressures of hydrogen are not used. For example, if the rate limiting step of the

conversion of ethylene to ethane is the hydrogenation of the ethyl intermediate shown in Fig. 1.1, it could be that with a H_2: C_2H_4 = 5 the ethyl intermediate dehydrogenates to ethylidene and then to ethylidyne. However with greater hydrogen: ethylene ratios (= 50) the reaction can easily proceed to the formation of ethane.

6.4. Conclusions.

The use of diluted gas mixtures and small hydrogen/ethylene ratios in the catalytic hydrogenation of ethylene on Pt (111) results in a surface nearly saturated with ethylidyne moieties, as revealed by the RAIRS spectra in Fig 6.1. The extent of this coverage is enough to hinder the hydrogenation of the olefin in the gas phase, causing a decrease in reaction probabilities. However, the use of a mixture with H_2:C_2H_4 = 50 under diluted conditions shows extensive ethylidyne removal, suggesting that the reaction takes place over a surface that is almost devoid of alkylidyne moieties, a trend that was not observed on the previous chapters of this work.

Taking into account the results from chapter 4, low ethylene pressures in the gas phase imply a switch in kinetics where the dissociative adsorption of hydrogen on the metal surface is no longer the rate-limiting step. This type of transition was expected from the experiments of this chapter. Nonetheless, the results from Fig. 6.1 seem to correlate, to some extent, with this switch in kinetics since they imply that employing diluted gas samples with H_2: C_2H_4 = 5 yields greater coverages of ethylidyne an effect that could be associated to the rate-limiting step of the mechanism of hydrogenation in the mTorr and sub mTorr pressure regime.

Further analysis of these diluted systems was hindered by inherent instrumental limitations. A future redesign of the mixing system for the high-pressure reactor might be in order to attain better experimental reproducibility.

6.5. References.

[1] Zaera F., *Phys. Chem. Chem. Phys* **2013**, 15, 11988-12003.

[2] Ebrahimi M.; Simonovis J.P.; Zaera F., *J. Phys. Chem. Lett.* **2014**, 5, 2121-2125.

[3] Zaera F.; Somorjai G.A., *J. Am. Chem. Soc.* **1984***, 106,* 2288-2293.

[4] Cremer, P.S; Su, X.; Shen, Y.R.; Somorjai, G.A, *J. Am. Chem. Soc.* **1996**, *118***,** 2942-2949.

[5] Ohtani, T.; Kubota, J.; Kondo, J.N.; Hirose, C.; Domen, K, *J. Phys. Chem. B* **1999**, *103*, 4562-4565.

[6] Tillekaratne, A.; Simonovis, J.P.; López Fagúndez, M.; Ebrahimi, M.; Zaera, F., *ACS Catal.* **2012**, *2*, 2259-2268.

[7] Skinner, P.; Howard, M.W.; Oxton, I.A.; Kettle, S.F.A.; Powell, D.B.; Shepard N., *J. Chem. Soc., Faraday Trans. II* **1981**, *77*,1203-1215.

CHAPTER 7: GENERAL CONCLUSIONS

The implementation of the operando setup described in this work was successful in confirming previous findings regarding the adsorption of strongly bonded hydrocarbon deposits, namely ethylidyne, on the Pt (111) surface during the high-pressure catalytic hydrogenation of ethylene. This unique setup also provided the means to modify experimental conditions to decouple the relation between the gas-phase olefin and the alkylidyne that is adsorbed during reaction. Furthermore, it enabled the in-situ exploration of the HD production kinetics, revealing an unprecedented behavior. Also, despite some issues associated with working in the mTorr pressure range, it was possible to determine that under these particular conditions the reaction occurs over a seemingly clean Pt surface.

In studying the role of strongly adsorbed hydrocarbon deposits it was confirmed that these alkylidyne moieties act as spectator species during the hydrogenation of ethylene over Pt, since they are hydrogenated at a slower rate than the gas-phase ethylene. It was also found that if the surface is pre-covered with a heavier hydrocarbon the rate of ethylene hydrogenation decreases. However, this surface effect seem to be fleeting, since the rates of reaction over butylidyne/Pt (111) and toluene/Pt (111) seem to display small rate increases that might be due to the displacement of the initial hydrocarbon adlayer. In addition, it was determined that the thermal decomposition of these pre-covered surfaces under UHV conditions seems to reshape the carbonaceous

adlayer, increasing the number bare Pt sites for catalysis, since there is a direct correlation between increasing temperatures and increasing ethylene hydrogenation rates.

While probing the dissociative adsorption of hydrogen as the rate-limiting step in the hydrogenation reaction of ethylene on Pt, it was determined that, for the experimental conditions used, the HD production reaction displayed non-linear kinetics, a surprising behavior that has not been reported before. It was interesting to find that the spike in HD production rate occurs before the hydrogenation of ethylene has been completed, a revelation that is counter-intuitive. Our results show that this phenomenon is a general trend, however it is easier to observe under reaction conditions where the H_2: C_2H_4 is relatively high, as is our case (H_2: C_2H_4 = 25). A close inspection of this behavior, found that the so-called spike in the HD accumulation is strongly dependent on the pressure of gas-phase ethylene, and it consistently occurs when the remaining pressure of the olefin is below 1 Torr. Furthermore, it was also shown that the HD spike is reversible, since the addition of a fresh batch of ethylene slows down the HD production reaction again. Adding this discovery to the first-order dependence on hydrogen displayed by the hydrogenation reaction of ethylene on Pt, and to the almost parallel evolution of HD and ethane accumulation, shows that the dissociative adsorption of H_2 on the transition metal surface is the rate-limiting step of the reaction in the stage before the sharp transition in HD production. After this switch in kinetics the H-D scrambling and the conversion of ethylene seem to progress independently suggesting a different rate-limiting step. This observation clearly defines two separate kinetic regimes in the hydrogenation of ethylene over Pt (111) surfaces. It is worth mentioning that a surface-site dependence of the H-D

production rate spike cannot be completely disregarded without further experimental evidence, since, regretfully, site specific blocking experiences with sulfur were inconclusive. Further experimentation is required in this particular area.

Finally, some progress was made in studying the pressure gap between high-pressure and UHV experiments. The low intensity of the ethylidyne umbrella deformation mode in the IR spectra of chapter five suggests that under these conditions the reaction takes place over a seemingly clean Pt surface and show an increase in the conversion rate of ethylene to ethane, demonstrating that lower ethylidyne coverages increase reaction probabilities. Comparison of these results with the reaction probabilities from molecular beam studies carried by our group for the same system seem to be in good agreement with this discovery.

APPENDIX 1: ESTIMATION OF CARBONACEOUS SURFACE COVERAGE THROUGH ADLAYER OXIDATION FOLLOWED WITH TEMPERATURE PROGRAMED DESORPTION.

A.1. Procedure and Results.

Given the nature of the resulting surfaces from the experiments carried out in this work, an attempt was made to develop a way to estimate the surface coverages of hydrocarbons by mean of TPD. This analysis consisted in carrying out the thermal oxidation of the hydrocarbon deposits in the UHV end of the chamber under 2 x 10^{-8} Torr of oxygen and ramping the temperature up to 750 K. The results of this analysis are shown in Figure A1. The determination of surface coverage should be related mostly to the evolution seen in the 44 (CO_2) and 28 (CO) amu traces, which follow the expected oxidation products.

Figure A1 shows no evolution of the indicated masses, even though the conditions for oxidation should be favorable in the presence of the excess oxygen. Presently, we still have not been able to determine the source of this inconsistency. Due to this fact, carbonaceous surface coverages were estimated solely with RAIRS.

Also, an unexpected signal trace is observed during the oxidation process at 29 amu. It is believed that this feature is an experimental artifact.

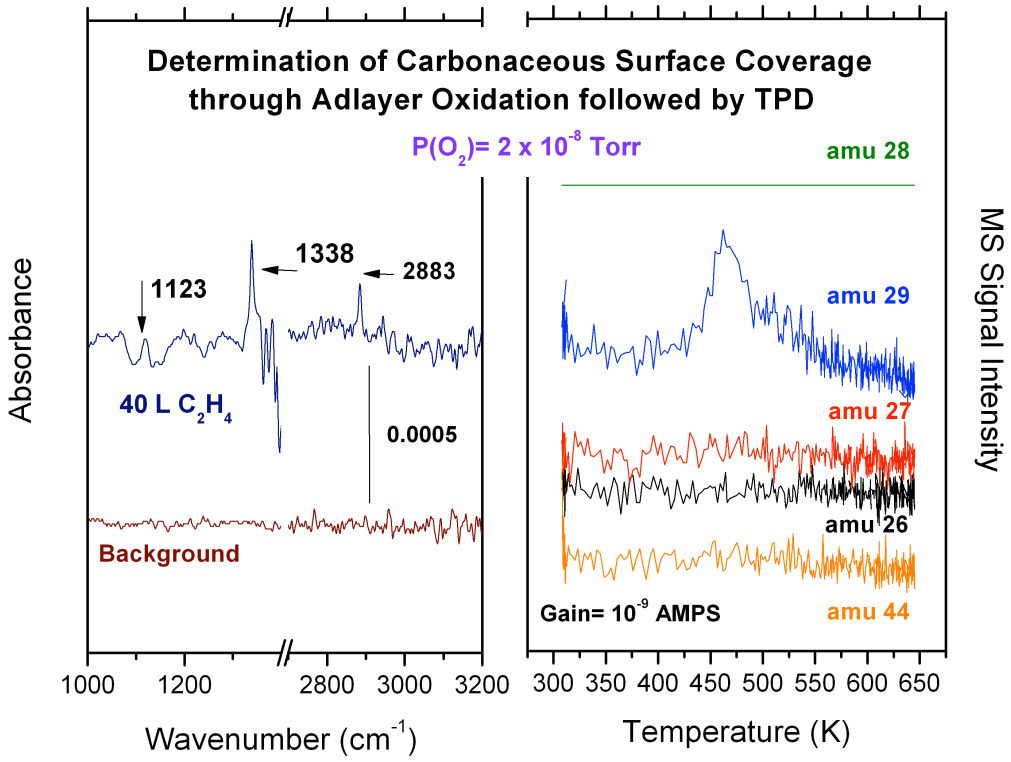

Figure A1. Attempt to determine the carbonaceous coverages via adlayer oxidation followed by TPD. Left: RAIRS spectrum of the saturated ethylidyne layer used for the TPD analysis. Right: TPD analysis in the presence of $2x10^{-8}$ Torr.

APPENDIX 2: PROCEDURE FOR DECONVOLUTING THE RAW MS DATA.

A2. Procedure and Results.

This appendix illustrates the general procedure to deconvolute the raw data obtained from the mass spectra. This was mostly needed in chapter 5 since the MS signals of ethane had contributions from its deuterated counterparts and vice versa. The approach employed here was a matricial analysis based on the following steps (This procedure is found in reference [5] of chapter 3):

1. The assembly of a square matrix $\mathbf{S} = [S_{ij}]$ that contains the mass spectrometer sensitivity factors S_{ij} of all compounds i and masses j to be recorded in the MS experiment.
2. The construction of a vector $\mathbf{I}(t) = [I_j(t)]$ for every time point in MS data with the mass spectrometry signal intensities I_j measured for each mass j.
3. The calculation of the partial pressures $\mathbf{P}(t)$ of each compound by carrying out the product $\mathbf{P}(t) = \mathbf{I}(t)*\mathbf{S}^{-1}$, where $\mathbf{S}^{-1}$ in the inverse of the sensitivity matrix $\mathbf{S}$. This is based on the assumption that the partial pressure of each compound at a given temperature $P_i(t)$ can be grouped into a vector $\mathbf{P}(t) = [P_i(t)]$ so that $\mathbf{I}(t) = \mathbf{P}(t)*\mathbf{S}$.
4. Step 3 was repeated for each vector $\mathbf{I}(t) = [I_j(t)]$ obtained for each time in the MS. This resulted in a matrix $\mathbf{M} = [P_{it}]$ consisting of a set of vectors $\mathbf{P}(t) = [P_i(t)]$, one for each time point.
5. Finally the vectors $\mathbf{P}(i)$ are plotted as a function of time, taking into consideration that the matrix obtained in step 4 can also be viewed as a collection of vectors $\mathbf{P}(i)$

= [P_t(i)] (the transpose of matrix **M**). This way, one MS trace is obtained fro each product *i.*

The deconvolution of the ethane product traces from typical experiment of chapter 5 are offered as an example in Figure A2. In this case five main masses were followed: 26 amu (C_2H_4), 29 amu (C_2H_3D), 30 amu (C_2H_6), 31 amu (C_2H_5D) and 22 amu ($C_2H_4D_2$).

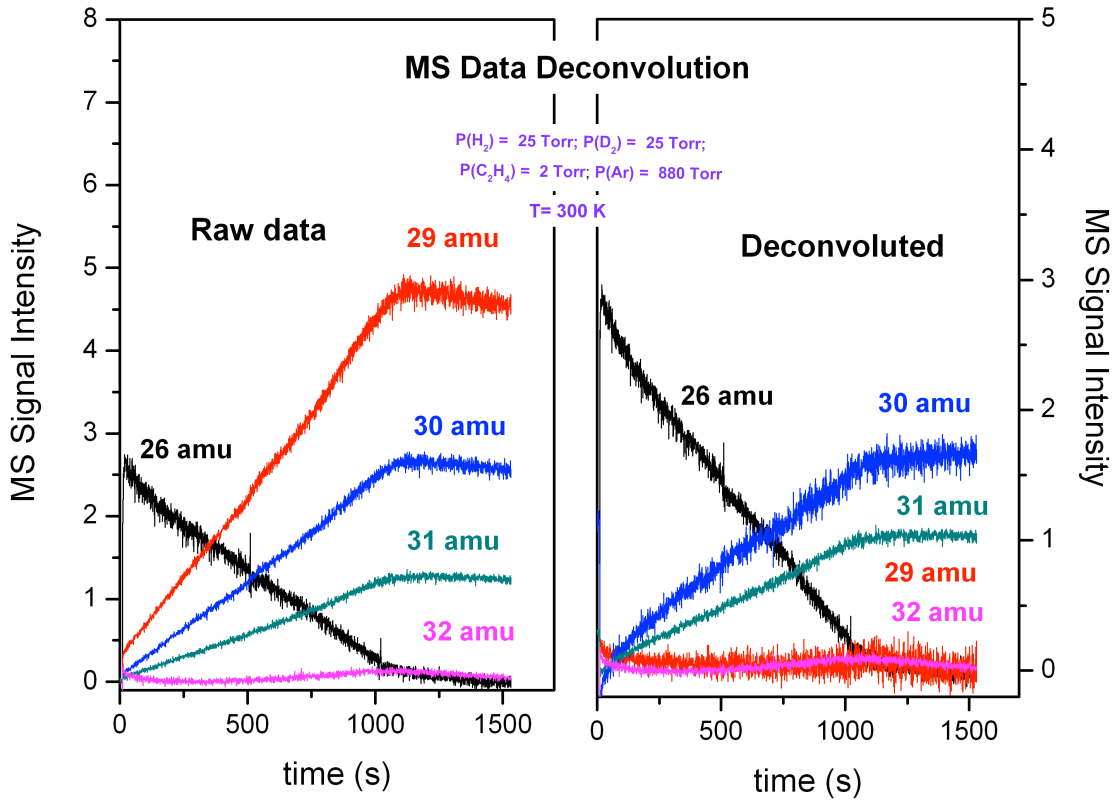

Figure A2. Deconvolution procedure for a typical experiment from chapter 5. Left: Raw data. Right: Deconvoluted data.